NAVAL POSTGRADUATE SCHOOL

MONTEREY, CALIFORNIA

THESIS

INTEGRATING COORDINATED PATH FOLLOWING ALGORITHMS TO MITIGATE THE LOSS OF COMMUNICATION AMONG MULTIPLE UAVs

by

Kyungnho Kim

March 2013

Thesis Advisor: Raymond R. Buettner
Co-Advisors: Vladimir N. Dobrokhodov
Kevin D. Jones

Approved for public release; distribution is unlimited

THIS PAGE INTENTIONALLY LEFT BLANK

REPORT DOCUMENTATION PAGE			Form Approved OMB No. 0704-0188
Public reporting burden for this collection of information is estimated to average 1 hour per response, including the time for reviewing instruction, searching existing data sources, gathering and maintaining the data needed, and completing and reviewing the collection of information. Send comments regarding this burden estimate or any other aspect of this collection of information, including suggestions for reducing this burden, to Washington headquarters Services, Directorate for Information Operations and Reports, 1215 Jefferson Davis Highway, Suite 1204, Arlington, VA 22202-4302, and to the Office of Management and Budget, Paperwork Reduction Project (0704-0188) Washington DC 20503.			
1. AGENCY USE ONLY ***(Leave blank)***	**2. REPORT DATE** March 2013	**3. REPORT TYPE AND DATES COVERED** Master's Thesis	
4. TITLE AND SUBTITLE INTEGRATING COORDINATED PATH FOLLOWING ALGORITHMS TO MITIGATE THE LOSS OF COMMUNICATION AMONG MULTIPLE UAVs		**5. FUNDING NUMBERS**	
6. AUTHOR(S) Kyungnho Kim			
7. PERFORMING ORGANIZATION NAME(S) AND ADDRESS(ES) Naval Postgraduate School Monterey, CA 93943-5000		**8. PERFORMING ORGANIZATION REPORT NUMBER**	
9. SPONSORING /MONITORING AGENCY NAME(S) AND ADDRESS(ES) N/A		**10. SPONSORING/MONITORING AGENCY REPORT NUMBER**	
11. SUPPLEMENTARY NOTES The views expressed in this thesis are those of the author and do not reflect the official policy or position of the Department of Defense or the U.S. Government. IRB Protocol number: N/A.			
12a. DISTRIBUTION / AVAILABILITY STATEMENT Approved for public release; distribution is unlimited		**12b. DISTRIBUTION CODE**	

13. ABSTRACT (maximum 200 words)

The thesis addresses the problem of mid-air collision avoidance among multiple Autonomous Unmanned Aerial Vehicles (UAVs) capable of communicating their flight states across a time-varying communication network. The UAVs' capabilities to (a) follow a given path and to (b) exchange and coordinate their relative position while on the path are considered the key factors enabling the time-critical coordination that in turn guarantees the safety of flight. The thesis is based on the key results of the recently developed concept of Coordinated Path Following (CPF) for multiple autonomous agents. While the path-following methodology is adapted without modification, the information exchange over the time-varying communication network and its impact on the performance of coordination was analyzed in a comparative study. The impact of the time-varying information flow is represented by the loss of link ratio, which is the ratio of time without information exchange to the nominal timeframe of communication in a given bidirectional network. The particular coordination metrics utilized are the coordination error (difference between the relative positions of UAVs on the paths) and the Euclidian distance between the UAVs (space separation). On the other hand, the control effort necessary to achieve the desired coordination is represented by the level and variation of the commanded velocity profile. The particular goal of the numerical study was to understand the amount of control effort required to achieve the desired separation of UAVs capable of exchanging a minimum number of parameters over a degrading communication network.

14. SUBJECT TERMS Unmanned Aerial Vehicle, Situational Awareness, Loss Link, SAA (Search and Avoid), MATLAB, SIMULINK, Safety Assurance Mechanism			**15. NUMBER OF PAGES** 75
			16. PRICE CODE
17. SECURITY CLASSIFICATION OF REPORT Unclassified	**18. SECURITY CLASSIFICATION OF THIS PAGE** Unclassified	**19. SECURITY CLASSIFICATION OF ABSTRACT** Unclassified	**20. LIMITATION OF ABSTRACT** UU

NSN 7540-01-280-5500 Standard Form 298 (Rev. 2-89)
Prescribed by ANSI Std. 239-18

THIS PAGE INTENTIONALLY LEFT BLANK

Approved for public release; distribution is unlimited

INTEGRATING COORDINATED PATH FOLLOWING ALGORITHMS TO MITIGATE THE LOSS OF COMMUNICATION AMONG MULTIPLE UAVs

Kyungnho Kim
Lieutenant, United States Navy
B.S., KyungNam University, 1998

Submitted in partial fulfillment of the
requirements for the degree of

MASTER OF SCIENCE IN INFORMATION TECHNOLOGY MANAGEMENT

from the

NAVAL POSTGRADUATE SCHOOL
March 2013

Author: Kyungnho Kim

Approved by: Raymond R. Buettner
Thesis Advisor

Vladimir N. Dobrokhodov
Thesis Co-Advisor

Kevin D. Jones
Thesis Co-Advisor

Dan C. Boger
Chair, Department of Information Science

THIS PAGE INTENTIONALLY LEFT BLANK

ABSTRACT

The thesis addresses the problem of mid-air collision avoidance among multiple Autonomous Unmanned Aerial Vehicles (UAVs) capable of communicating their flight states across a time-varying communication network. The UAVs' capabilities to (***a***) *follow a given path* and to (***b***) *exchange* and *coordinate* their relative position while on the path are considered the key factors enabling the time-critical coordination that in turn guarantees the safety of flight. The thesis is based on the key results of the recently developed concept of Coordinated Path Following (CPF) for multiple autonomous agents. While the path-following methodology is adapted without modification, the information exchange over the time-varying communication network and its impact on the performance of coordination was analyzed in a comparative study. The impact of the time-varying information flow is represented by the loss of link ratio, which is the ratio of time without information exchange to the nominal timeframe of communication in a given bidirectional network. The particular coordination metrics utilized are the coordination error (difference between the relative positions of UAVs on the paths) and the Euclidian distance between the UAVs (space separation). On the other hand, the control effort necessary to achieve the desired coordination is represented by the level and variation of the commanded velocity profile. The particular goal of the numerical study was to understand the amount of control effort required to achieve the desired separation of UAVs capable of exchanging a minimum number of parameters over a degrading communication network.

THIS PAGE INTENTIONALLY LEFT BLANK

TABLE OF CONTENTS

I. INTRODUCTION 1
- **A. BACKGROUND 1**
- **B. MOTIVATION 3**
- **C. PROBLEM STATEMENT 7**
- **D. PROPOSED APPROACH 7**

II. ENABLING TECHNOLOGIES 9
- **A. ARCHITECTURE 9**
- **B. DECOUPLING SPACE AND TIME 11**
- **C. TRAJECTORY GENERATION 12**
  - **1. Trajectory Generation for Single UAVs 12**
  - **2. Trajectory Generation for Multiple Vehicles 14**
    - ***a. Collision Avoidance in Space 15***
    - ***b. Collision Avoidance in Time 16***
- **D. PATH FOLLOWING 16**
- **E. TIME COORDINATION 18**
- **F. COORDINATION LAW 20**
- **G. INFORMATION EXCHANGE ARCHITECTURE 21**
  - **1. Basic Definition 21**
    - ***a. Adjacency Matrix 22***
    - ***b. Degree Matrix 22***
    - ***c. Laplacian Matrix 22***
    - ***d. Practical Examples 23***
    - ***e. The Consensus Dynamic 24***
  - **2. Consensus Algorithm 25**
  - **3. Coordination Control Law 25**
- **H. SPACE AND TIME SEPARATION EXAMPLE 26**
  - **1. Example of Collision Avoidance in Time 26**
  - **2. Example of Collision Avoidance in Space 27**

III. IMPLEMENTATION OF THE COORDINATED PATH FOLLOWING 29
- **A. DIAGRAM OVERVIEW 29**
- **B. UAV AND AUTOPILOT 30**
- **C. PATH FOLLOWING CONTROLLER 31**
- **D. COORDINATION CONTROLLER 32**
  - **1. Implementation of Consensus Algorithm 32**
    - ***a. Simulation Result of the Consensus Algorithm without the PI Controller 33***
    - ***b. Simulation Result of the Consensus Algorithm with the PI Controller 34***
  - **2. Coordination Controller 35**

IV. EXPERIMENTAL RESULTS 37
- **A. DESIGN OF THE EXPERIMENT 37**

1. Simulation Setup 38
2. Ideal Communication Condition with Non-Zero Coordination Reference 42
3. Variation of the Communication Conditions 44
B. OVERVIEW OF NUMERICAL RESULTS 47
V. CONCLUSION AND FUTURE WORK 49
A. CONCLUSION 49
B. FUTURE WORK 50
C. RECOMMENDATION 50
LIST OF REFERENCES 53
INITIAL DISTRIBUTION LIST 57

LIST OF FIGURES

Figure 1. The number of mishaps between UAVs and Manned Aircraft in military. Adapted from "U.S. Unmanned Aerial Systems," by J. Gertler, 2012. The figure demonstrates the significance of mishaps between military UAVs and military manned aircraft. 4
Figure 2. The hierarchy structure of CPF architecture. 10
Figure 3. Conceptual architecture of the cooperative control framework adapted from "Time-Critical Cooperative Control of Multiple Autonomous Vehicles," by Xargay et al., 2010. 11
Figure 4. Following a virtual target vehicle. 17
Figure 5. Geometry problem of two-dimensional PF..... 18
Figure 6. Example topology and the key matrixes. Three elements represent a UAV and the arrow represents the direction of communication. 23
Figure 7. Collision avoidance in time with two UAVs adapted from "Time-Critical Cooperative Control of Multiple Autonomous Vehicles," by Xargay et al., 2010. (a) Three-dimensional spatial paths, (b) Speed profiles, (c) Path separation, (d) Vehicle separation..... 27
Figure 8. Collision avoidance in space with two UAVs adapted from "Time-Critical Cooperative Control of Multiple Autonomous Vehicles," by Xargay et al., 2010. (a) Three-dimensional spatial paths, (b) Speed profiles, (c) Path separation, (d) Vehicle separation..... 28
Figure 9. CPF Model of two UAVs. The diagram demonstrates the top-level architecture of the model. 30
Figure 10. The UAV with autopilot Module. The module consists of autopilot and the 6 DOF-EOM modules. 31
Figure 11. The CPF Controller. 32
Figure 12. Practical implementation of consensus algorithm, discussed in Figure 6. 33
Figure 13. The simulation result of the consensus algorithm without the PI controller. The initial condition is assigned at 10m, 50m, and 100m. The final states converge to a median value instead of zero. 34
Figure 14. The simulation result of the consensus algorithm with the PI controller. The initial condition is assigned at 10m, 50m, and 100m. The coordination is achieved in approximately 0.5 second. 35
Figure 15. Simulink diagram that implements the time critical cooperative coordination control law. 36
Figure 16. Results of simulating 2 UAVs following symmetric paths. Note that the scales along the axis are not the same. 40
Figure 17. Coordination parameters in symmetric setup under lossless communication conditions. 41
Figure 18. Simulink implementation of non-zero coordination reference. 43
Figure 19. Result of coordination under ideal communication and non-zero coordination reference. 44
Figure 20. Simulink implementation of the loss of communication scheduler. 45

Figure 21. Impact of the communication loss on coordination performance. 46
Figure 22. Control efforts expressed in terms of desired speed profile. 47

LIST OF TABLES

Table 1. Class A mishap rate per 100,000 flight hours. Adapted from "Unmanned Aerial Vehicles and uninhabited Combat Aerial Vehicles," by DoD, 2004. 5
Table 2. Cause of UAV Mishap. Adapted from "Unmanned Aerial Vehicles and uninhabited Combat Aerial Vehicles," by DoD, 2004. 6
Table 3. Parameters of the symmetric simulation. 39

THIS PAGE INTENTIONALLY LEFT BLANK

LIST OF ACRONYMS AND ABBREVIATIONS

2D	Two Dimensional
3D	Three Dimensional
CPF	Coordinated Path Following
DOF	Degree Of Freedom
EOM	Equations of Motion
FAA	Federal Aviation Administration
GCS	Ground Control Station
MAC	Mid-Air Collision
NAS	National Airspace System
PF	Path Following
SA	Situational Awareness
UAS	Unmanned Aerial System
UAV	Unmanned Aerial Vehicle

THIS PAGE INTENTIONALLY LEFT BLANK

ACKNOWLEDGMENTS

If not for the assistance and support of the following people, this thesis work would have been much more difficult, or impossible to accomplish.

At NPS, I would first like to thank my advisor Professor Buettner, Professor Dobrokhodov, and Professor Jones for giving me a chance, for inviting me to get started on such an interesting problem, for providing me with excellent discussions about modeling and simulation, and for giving selfless support through education and research. I would like to thank Mr. Jeff Wurz for reviewing my draft and answering numerous questions on Mathwork Simulink. Finally, I have to thank the IST department, especially Mr. Cook and Mr. Roberts, for their unfailing patience and guidance.

At home, I have to thank my family for their confidence and constant support. Especially, I would like to thank Heejin for absolutely everything.

THIS PAGE INTENTIONALLY LEFT BLANK

I. INTRODUCTION

A. BACKGROUND

Today, National Airspace System (NAS) provides one of the safest means of air transportation and the fastest-growing business environment. The primary customer of the national airspace system is not only the domestic and international passenger group, but also the commercial air carrier, general aviation, and non-commercial aviation. It is estimated that the capacity of the national airspace is approaching its limits; however, the air traffic will continue to increase. For example, the Federal Aviation Administration (FAA) forecasts that the industry will grow from 731 million passengers in 2011 to 1.2 billion in 2032, which does not consider general aviation, unmanned aviation, and other segments (DOT, 2012).

Recent rapid advances in unmanned technologies bring to a consideration the Unmanned Aircraft Systems (UAS) as another significant customer of the same airspace. UAS comes in a variety of shapes and sizes, and serves a variety of purposes. Some of them have wingspans as small as a few centimeters, while the others have wingspans as large as the Boeing 737 (DOT, 2012). The FAA (DOT, 2012) believes that over 50 companies, universities, and government organizations are developing and producing approximately 155 unmanned aircraft designs. The FAA forecasts an annual growth of 12% for the UAS military market and over $94 billion in total UAS spending over the next 10 years, therefore adding up to roughly 10,000 active commercial UASs in five years (DOT, 2012). In accordance with the Joint Planning and Development Office (JPDO) report, industry projections for 2018 forecast more than 15,000 UAS in service in the U.S., with a total of almost 30,000 deployed worldwide. Consequently, the capacity of the national airspace might be reaching its limits much sooner than initially projected.

Unmanned Aerial Vehicles (UAVs) continue to increase their importance in a broad range of applications. They are by far the fastest-growing segment of the military-oriented aeronautical industry. The Weibel & Hansman (2005) report observes that the recent technological advancements and increased military utilization have proven the

operational viability of UAVs and made them attractive for a wide range of potential civil and commercial applications. However, in general, the cost of a very capable UAV is much cheaper than the risk of any human-related incident. On the other hand, UAVs are capable of performing risky tasks that humans are either incapable of doing or that are too dangerous to perform, depending on the hostility of the environment. The examples include a variety of military surveillance, fire monitoring, traffic patrolling, and scientific observations. Yet, a great number of UAS will be emerging to operate in the same national airspace system in the near future.

Today, over 731 million passengers have to share the same national airspace with a continuously increasing number of UAS. Since the capacity of airspace is limited, maintaining the safety in NAS becomes more challenging. The primary reasons for the complexity are twofold. On the one hand, the density and sophistication of ever-increasing "manned" air traffic requires significant changes in air traffic control. On the other hand, the steady growth of Unmanned Aerial Systems (UAS) demands its own live space from the same NAS volume. From an operational, infrastructure, and safety perspective, this presents a number of challenges. Among them, the safety assurance is considered one of the primary concerns in the NAS in the nearest future. With safe integration into the airspace, UAS has the potential to be a significant and valuable component in commercial aviation.

Scientists are perfecting a number of the technologies to enable a safe operation of UAVs in the air. Nevertheless, almost all classes of UAVs pose significant challenges to the safety of airspace operation, leading to significantly increased probabilities of Mid Air Collision (MAC) that is primarily a result of their inherent SWAP (Size, Weight and Power) limitations (Contarino, 2009). Although rapidly evolving in every direction, the current state of the art of onboard communication, power and sensor technologies, radar, acoustic sensing, and Electro-Optical Infrared sensor still result in hitting the SWAP constraints. Quite often the resulting solutions are extremely expensive and/or still immature enough to deliver the performance necessary for safe autonomous operation in typical, modern applications of unmanned technologies.

Furthermore, the volume of the UAV operations is increasing significantly due to its high effectiveness and demand. The growth of UAV traffic in the confined national airspace consequently increases the probability of MAC. With the inherent SWAP limitation, the operation of immature UAVs in the same national airspace system can be the biggest threat in the safety of the national airspace system.

The operation of UAVs depends heavily on Situational Awareness (SA), currently maintained and provided on the ground by the onboard instrumentation and communication links. Regardless of the situation, a failure in providing SA can result in an unacceptable and unrecoverable MAC. A loss of the primary command and control link, along with the utility links, is the primary contributing factor to the effectiveness of SA. The loss of link can be defined as a failure to communicate critical information among the airborne vehicles and the corresponding Ground Control Stations (GCS). An analysis of loss of link conditions and the development of means of preventing it can be one of the primary milestones in the design of a collision-free assurance mechanism.

B. MOTIVATION

The research in this thesis began with a question: How much adverse impact can be expected when UAS emerges into the same national airspace in the near future? On the safety aspect, a mishap rate delivers important information, such as the reliability of the system, the current technology, the probability of MAC, and the causes of mishaps. In an attempt to address these safety issues, researchers all over the world are developing a number of safety-critical technologies, including the collision avoidance algorithms. These efforts have already significantly improved the reliability of modern UAV systems. However, the historical data indicates that the current level of UAS technologies still has room for improvement. Increasing the number of vehicles in airspace at a given time will increase the probability of collision between vehicles in the same air volume. Any incident in national airspace is unacceptable.

The amount of adverse impact can be estimated from the previous mishap rate and mishap comparison among military manned aircraft, commercial aircraft and UAVs. Figure 1 presents the rate of mishap per 100,000 flight hours that occurred in 2005,

comparing the number of mishaps between unmanned and manned aircraft. In 2005, two military-manned aircraft such as the U-2 and F-16 demonstrated a fairly low mishap rate as 6.8 mishaps and 4.1 mishaps per every 100,000 flight hours. But, the most advanced military UAV system, currently carrying important missions, displays a much higher mishap rate, i.e., 20 incidents for Predator, and 88 incidents for Global Hawk per every 100,000 flight hours of the operations. The mishap ratio between manned aircraft and unmanned system is as high as 1 to 68.5. Figure 1 clearly illustrates that an unmanned system in the same operational environment has a potentially higher probability of incident, which can be integrated in the probability of MAC.

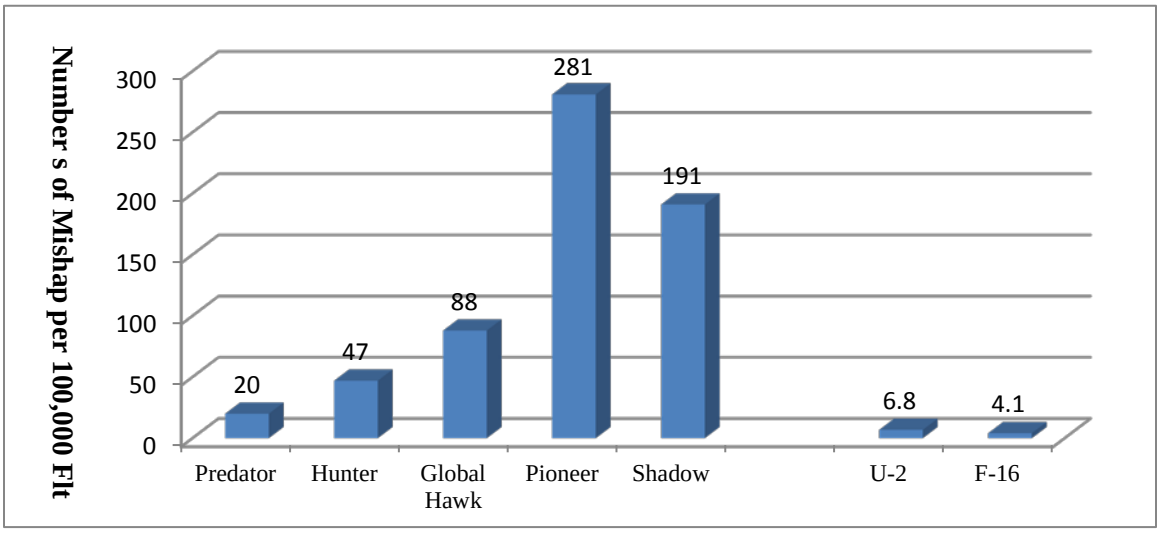

Figure 1. The number of mishaps between UAVs and Manned Aircraft in military. Adapted from "U.S. Unmanned Aerial Systems," by J. Gertler, 2012. The figure demonstrates the significance of mishaps between military UAVs and military manned aircraft.

Table 1 compares the Class A mishap among military UAV systems, general aviation, regional commuter, and large airliners. Class A mishap is defined as "the resulting total cost of damages to Government and other property is $2 million or more, a DoD aircraft is destroyed (excluding UAS Groups 1, 2, or 3), or an injury or occupational illness results in a fatality or permanent total disability" (USD AT&L, 2011). The table counts only the worst mishap incidents and delivers the probability of the worst cases. Therefore, Table 1 provides a snapshot of the risk of a UAV's operation when a UAV

system enters into a commercial airspace. Assuming that an aircraft flies for 20 hours per day, and 25 days of operation per month, the first accident would occur after 1,600 years. On the other hand, an unmanned vehicle Pioneer will get the first mishap in every 229 flight hours, which means once every 11 days in the same operational condition. It is so obvious that an unmanned system displays the higher probability than a manned aircraft. Table 1 provides a picture of probability of MAC when they share the same air space. In fact, large airliners would not be able to maintain as low as 0.01 mishap rate per 100,000 flight hours unless a UAV improved its mishap rate.

UAV Mishaps	**Aircraft Mishaps**
Predator: 32*	F-16: 3
Pioneer: 334*	General Aviation: 1
Hunter: 55*	Regional Commuter: 0.1
* much less than 100,000 flight hours	Large Airliners: 0.01

Table 1. Class A mishap rate per 100,000 flight hours. Adapted from "Unmanned Aerial Vehicles and uninhabited Combat Aerial Vehicles," by DoD, 2004.

Obviously, a significant level of adverse impact can be expected when the current UAV system merges into today's commercial airspace. Safety in the national airspace system is everyone's primary objective. To achieve any improvement of UAV mishap, it is important to analyze the causes of UAV mishaps. Table 2 categorizes the cause of UAV mishap of Table 1. Defense Science Board (DoD, 2004) identifies five categories of UAV mishap causes such as power and propulsion, flight controls, human error, communication, and miscellaneous. By improving technologies and system design, most of the mechanical errors, such as flight controls and power and propulsion, can be eliminated in the near future. Human error and communication issues will be avoided by improving the design and robustness of the communication network between UAVs, and between UAVs and human operators on the ground.

UAV MISHAP CAUSE	PERCENT
Power and Propulsion	37 %
Fight Controls	25 %
Human Error	17 %
Communications	11 %
Miscellaneous	10 %

Table 2. Cause of UAV Mishap. Adapted from "Unmanned Aerial Vehicles and uninhabited Combat Aerial Vehicles," by DoD, 2004.

Due to the importance and capacity limitation of the National Airspace system, the safety of NAS is the nation's top priority. In fact, some federal agencies have already begun research into the safety of NAS. Moreover, as the highest authority, President Barack Obama, in February 2012, ordered and signed legislation directing the Federal Aviation Administration to develop a plan by September 30, 2015, for integrating civil unmanned aerial vehicles into NAS (McGarry, 2012). The FAA is eager to solve the national airspace capacity problem to maintain the NAS as safe as possible. After performing significant research in this area, the FAA published the reports related to forecasts of capacity needs in the national air space. Also, the FAA collects and analyzes any UAV-related data and reflects on the Aerospace forecast report. NASA is interested in integrating UAVs in the National Airspace System. The current topics of concern are Separation Assurance for small UAS, and small UAS trajectory planning in non-positively controlled airspace.

As a result, the key motivation of this thesis is to review the current airspace capacity, analyze the importance of emerging UAVs in the National Airspace System, and propose an approach that can guarantee safe and predictable behavior of multiple heterogeneous aircrafts in the same airspace. The research will improve the reliability and responsiveness of UAVs, which directly contribute to the safety of the national airspace system.

C. PROBLEM STATEMENT

Communication with GCS and among the airborne vehicles is among the most critical factors in the flight safety of multiple aerial vehicles in the constraint airspace. It is intuitive, and it has been proven in operation of multiple aircrafts that in a situation when a UAV loses its ability to communicate either with a human operator or with other aerial vehicles in the same airspace, the probability of MAC rises significantly. Therefore, the ability of aircrafts to stay on the assigned path and to communicate their current status—such as position, velocity, attitude, and possibly their intent—are the key enabling solutions of the collision-free flight.

The primary objective of the thesis is to develop a solution of the collision-free flight of multiple UAVs under given specific conditions. The conditions of interest include the confined airspace, limited and time-varying communication among autonomous vehicles, and the flight dynamics limitations of tactical UAVs. Moreover, the realistic modeling of UAV's flight dynamics is another important and challenging task. As a result, to facilitate the solution of time-critical coordination problem, the thesis considers the following tasks:

- Define the architecture of onboard algorithms addressing the problem of precise path following (PF) and coordination among multiple UAVs operating in the same confined airspace.
- Define the algorithms enabling the PF and coordination capabilities.
- Evaluate an impact of the intermittent loss of communication among UAVs on the performance of coordination.
- Propose a solution to MAC in a situation where the coordination is impaired by the severe loss of communication.

D. PROPOSED APPROACH

To facilitate the solution of the collision-free flight of multiple UAVs, this thesis considers the problem of automatic control of multiple cooperative UAVs operating in confined airspace in the presence of intermittent communication links and realistic flight dynamics of aircraft. Conceptually the work proposes and considers two possible solutions to the collision-free flight: first is the separation of UAVs in space—when there are no intersecting trajectories; and second is the separation of UAVs in time—when

there are intersections, although the airplanes communicate their position states in order to avoid collisions by adjusting their speed along the path. In particular, the work considers two types of tasks defined at single and multiple aircraft levels. At the single aircraft level, the key enabling block is the task of precise PF. At the multiple aircraft level, the enabling algorithms include the collision-free path generation and the coordinated PF. The key to the success of the proposed solution is to develop a robust communication network among autonomous vehicles in a time-critical cooperative control environment.

II. ENABLING TECHNOLOGIES

A. ARCHITECTURE

To achieve the goal of collision-free simultaneous flight of multiple autonomous vehicles in confined airspace, the required Coordinated Path Following (CPF) functionality of a single UAV should include the algorithms of PF and time coordination. Figure 2 presents the architecture of the (CPF) concept. The PF algorithm is designed to make an airborne vehicle converge to and follow a desired three-dimensional (3D) geometric path, without an explicit timing law associated with it. The PF algorithm also includes the algorithm of the path generation that defines the nominal desired path and speed profile of an airplane.

The path-generation algorithm generates a required path based on mission specifications that include the objectives to be achieved, the constraints (tactical and environmental) and limitations imposed by the flight dynamics and onboard mission payload sensor. When generating the 3D path that accounts for the mission objectives and satisfies all the constraints, the path-following capability allows a vehicle to follow a predefined path. Note that the control law for the PF focuses solely on the proper control of pitch and yaw rates while assuming that the airspeed is sufficient to sustain the flight. The issue of coordination arises as soon as the capabilities of a single UAV is not sufficient to achieve the mission objectives and more than one airplane is necessary; for example, a single UAV with the SWAP limitation is not able to carry multiple heavy sensors performing simultaneous observations in a single mission.

As a result, when a fleet of vehicles carries the same mission with the same or closely positioned path, the tight coordination among multiple vehicles is critical to the success of the mission. First, this might be required by the mission objectives; second, it is required by the guidelines for collision avoidance. Time coordination is designed to coordinate the simultaneous flight operation of multiple autonomous vehicles, sharing the same airspace without a collision.

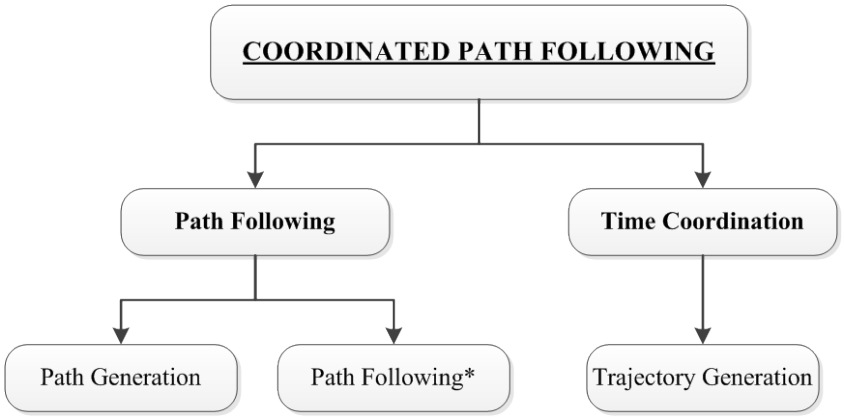

Figure 2. The hierarchy structure of CPF architecture.

Xargay et al. (2010) presents a successful implementation of the CPF architecture integrated on board of each UAV; see Figure 3. It can be observed that the control architecture exhibits a multi-loop control structure in which an inner-loop controller, called an autopilot, stabilizes the UAV dynamics, while a guidance outer-loop controller is designed to control the vehicle kinematics, providing PF and coordination capabilities. If the connectivity of the communication graph verifies a specific persistence of excitation-like conditions and the initial conditions are within a given domain of attraction, then the CPF capability can solve the time-critical cooperative PF problem with guaranteed rates of exponential convergence.

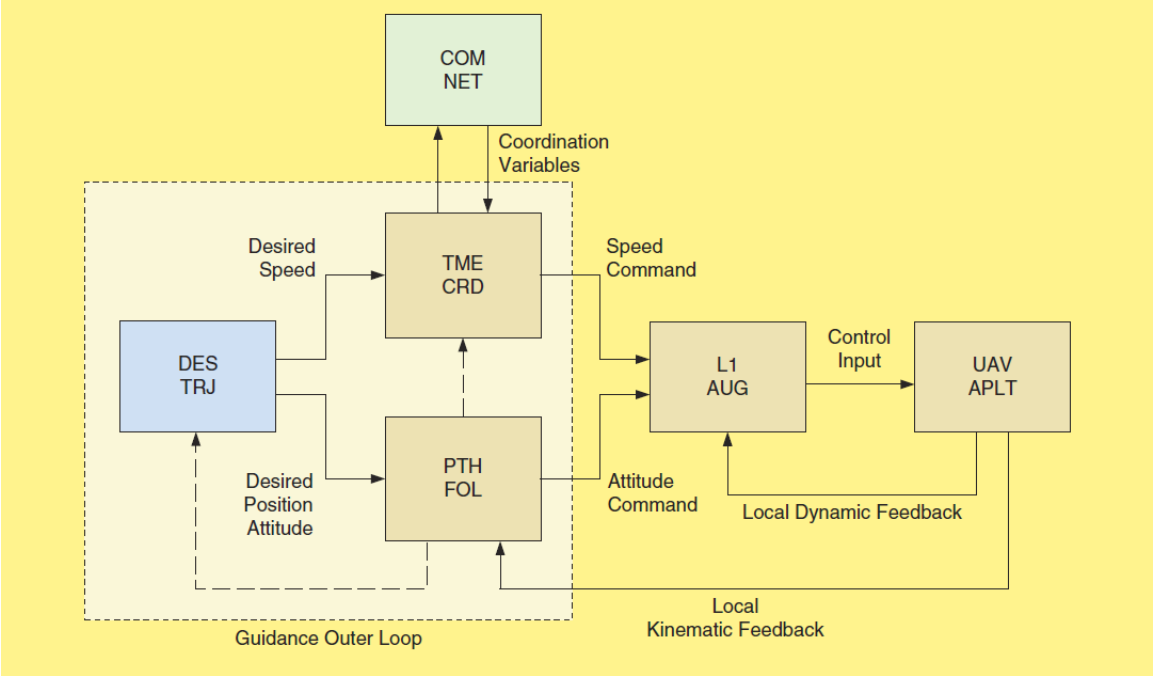

Figure 3. Conceptual architecture of the cooperative control framework adapted from "Time-Critical Cooperative Control of Multiple Autonomous Vehicles," by Xargay et al., 2010.

Therefore, this section addresses the contributing technologies and describes the control ideas that implement the desired capabilities. Each of the sections below addresses the following particular algorithms:

- Decoupling of space and time
- Trajectory generation
- Path following
- Time critical coordination
- Examples of collision avoidance in time and space

B. DECOUPLING SPACE AND TIME

The problem of coordinated control of multiple autonomous vehicles is to enable collision-free flight under strict spatial and temporal constraint. The decoupling of space and time provides a solution of the coordination problem. Unlike the term "trajectory," path is the continuous route of "positions" without considering a timing law associated with the position; this can be considered as an ability to define the same path and to

enable following the path with different speeds. Therefore, sharing the same airspace among a fleet of vehicles in the same mission raises a serious concern of a MAC. Every vehicle on the same path should be separated while maintaining a minimum safety distance threshold. Decoupling between space and time enables the separation of a three-dimensional path and speed profile associated with the path. The key idea of employing the concept of decoupling space and time can be summarized in the following basic steps. First, a set of feasible spatial paths with practical nominal speed profiles is generated for a fleet of vehicles that are assigned in the same mission. The second step ensures that a fleet of vehicle follows its assigned path—the PF step. Finally, the planned nominal speed profile of each individual vehicle obtained at the path generation step is executed by each UAV in the fleet, and the corresponding state (position) on the trajectory is "shared" over the communication network among the vehicles in the fleet. In turn, the velocity profile is continuously adjusted by each UAV to account for possible adverse disturbances, resulting in some or all UAVs not following the desired nominal speed profile. Obviously, the final step requires time coordination that, realistically, will also be a time-varying communication network because of possible communication failures and dropouts.

C. TRAJECTORY GENERATION

1. Trajectory Generation for Single UAVs

This section presents the conceptual idea of path generation and the steps required to implement the idea in software. In the current approach, a path is represented by an algebraic continuous function of a parameter τ; when $\tau=0$, the function output corresponds to the initial conditions of a UAV on the path while $\tau = 1$ gives the final coordination. A feasible trajectory generation algorithm considers a desired spatial path satisfying the mission performance metrics and also calculates the associated nominal speed profile. A set of parameters utilized in the path representation is as follows:

i-th vehicle's three-dimensional desired time trajectory: $p_{d,i}(t_d): R \to R^3$

the desired mission duration: t_d^*

the current mission time: $t_d \in [0, t_d^*]$

total length of the *i*-th vehicle's path: l_{fi}

position of *i*-th vehicles on the path length: $\tau_{li} \in [0, l_{fi}]$

Consider a task of defining a desired speed profile $v_{d,i}(t_d)$ corresponding to the desired duration of the mission t_d; note that t_d is the same for all UAVs in the fleet. A desired speed profile, $v_{d,i}(t_d)$ can be defined by the path length $\tau_{l,i}$ and the mission time t_d through the dynamic relation of the form $(d\tau_{l,i} / dt_d) = \theta_i(\tau_{l,i})$, where θ_i is a positive function, continuous and smooth in its argument. Therefore, the mission time t_d can be computed from the path length $\tau_{l,i}$:

$$t_d = \int_0^{\tau_{l,i}} \frac{1}{\theta_i(\sigma_\tau)} d\sigma_\tau \tag{1}$$

The following algebraic relations connecting geometric relations (curvature and torsion) of a path with the kinematic parameters (velocity and acceleration) of a UAV following the path are used in the definition of kinematics of a UAV assigned to the following path:

1. Vehicle's speed.

$$v_{d,i}(t_d(\tau_{l,i})) = \| p'_{d,i}(\tau_{l,i}) \| \theta_i(\tau_{l,i}), \tag{2}$$

where $p_{d,i}$ is a desired position of *i*-th UAV, $\tau_{l,i}$ is a path length of *i*-th vehicle, and θ_i is a positive function of *i*-th UAV.

2. Vehicle's acceleration

$$a_{d,i}(t_d(\tau_{l,i})) = \| p''_{d,i}(\tau_{l,i})\theta_i(\tau_{l,i}) + p'_{d,i}(\tau_{l,i})\theta'_i(\tau_{l,i}) \| \theta_i(\tau_{l,i}), \tag{3}$$

3. Curvature of the path

$$k_{d,i}(\tau_{l,i}) = \frac{\| p'_{d,i}(\tau_{l,i}) \times p''_{d,i}(\tau_{l,i}) \|}{\| p'_{d,i}(\tau_{l,i}) \|^3}, \tag{4}$$

4. Torsion of the path

$$\tau_{d,i}(\tau_{l,i}) = \frac{(p'_{d,i}(\tau_{l,i}) \times p''_{d,i}(\tau_{l,i})) \cdot p'''_{d,i}(\tau_{l,i})}{\| p'_{d,i}(\tau_{l,i}) \times p''_{d,i}(\tau_{l,i}) \|^2}, \tag{5}$$

5. Vehicle's flight path angle in terms of $p_{d,i}(t^d)$

$$\gamma_{d,i}(\tau_{l,i}) = \arctan\left(\frac{p'_{d,i}(\tau_{l,i}) \cdot \overrightarrow{e_{I3}}}{((p'_{d,i}(\tau_{l,i}) \cdot \overrightarrow{e_{I2}})^2 + (p'_{d,i}(\tau_{l,i}) \cdot \overrightarrow{e_{I2}})^2)^{1/2}} \right), \tag{6}$$

where the orthonormal vectors $\{\vec{e}_{I1}, \vec{e}_{I2}, \vec{e}_{I2}\}$ characterize an inertial reference frame $\mathcal{I}$. Now, the desired mission duration can be written.

$$t^*_d = \int_0^{l_{fi}} \frac{1}{\theta_i(\tau_{l,i})} d\tau_{l,i} \tag{7}$$

Based on the relations (2) - (6), a feasible trajectory can be generated when the constraints of maximum curvature, torsion and flight path angle bounds are satisfied. The constraints for a feasible trajectory can be expressed as:

$$0 < v_{\min} \le v_{d,i}(t_{d,i}(\tau_{l,i})) \le v_{\max} \tag{8}$$

$$| a_{d,i}(t_d(\tau_{l,i}) | \le a_{\max} \tag{9}$$

$$| k_{d,i}(\tau_{l,i}) | \le k_{\max} \tag{10}$$

$$| \tau_{d,i}(\tau_{l,i}) | \le \tau_{\max} \tag{11}$$

$$\gamma_{\min} \le \gamma_{d,i}(\tau_{l,i}) \le \gamma_{\max} \tag{12}$$

Thus, the trajectory is feasible if all of the conditions above are met for all $\tau_{li} \in [0, l_{fi}]$.

2. Trajectory Generation for Multiple Vehicles

Trajectory generation for multiple cooperative UAVs is a complicated task. From the requirements of trajectory generation for a single UAV, cooperative trajectories should consider another critical constraint that is a collision-free flight. Collision in the airspace can be avoided by separating trajectories in space and/or managing speed profile to achieve different times of arrival to the same 3D position. The solution of collision-free path generation is twofold. Collision can be avoided in space by ensuring that no feasible paths intersect. On the other hand, collision avoidance in time can be achieved by adjusting each vehicle's speed profile, which ensures that no two vehicles stay in the same (collision) space at the same time.

a. Collision Avoidance in Space

Collision avoidance in space can be achieved by adjusting the path; note that trajectory is the combination of path and velocity. In this case, the path generation algorithm should account for the fact that the position of each vehicle should maintain a certain proximity threshold that guarantees the spatial separation. A minimum allowable threshold (E) should be predetermined and verified by the flight performance of UAVs. Theoretically, collision avoidance in space can be achieved by maintaining a spatial distance between both vehicles simultaneously. This idea can be formally expressed in a mathematical form.

$$\min_{j,k=1,\ldots,n,\, j\neq k} \| p_{d,j}(\tau_{l,j}) - p_{d,k}(\tau_{l,k}) \|^2 \geq E^2, \text{for all } (\tau_{l,j}, \tau_{l,k}) \in [0, l_{fj}] \times [0, l_{fk}], \tag{13}$$

Let $\delta t^*_{d,i} \triangleq [t^*_{d\min,i}, t^*_{d\max,i}]$ be the arrival time window (allowable margin) for the i-th vehicle from the minimum mission duration to the maximum mission duration, where $t^*_{d\min,i}$, and $t^*_{d\max,i}$ represent the minimum and maximum possible mission duration for the i-th vehicle. Using the notations introduced above, the limits of the mission duration can be expressed as follows:

$$t^*_{d\min,i} \triangleq \frac{l_{fi}}{v_{\max}}, \text{ where } v_{\max} \text{ is a maximum UAV velocity and } l_{fi} \text{ is length of the mission} \tag{14}$$

$$t^*_{d\max,i} \triangleq \frac{l_{fi}}{v_{\min}}, \text{ where } v_{\min} \text{ is a minimum UAV velocity and } l_{fi} \text{ is length of the mission} \tag{15}$$

Therefore, the arrival margin is defined as:

$$\delta T^* \triangleq \min_i t^*_{d\max,i} - \max_i t^*_{d\min,i},\ i \in \{1,\ldots,n\} \tag{16}$$

Therefore, the cooperative path generation problem accounting for the collision avoidance in space can be re-written as:

$$\min_{j,k=1,\ldots,n,\, j\neq k} \| p_{d,j}(\tau_{l,j}) - p_{d,k}(\tau_{l,k}) \|^2 \geq E^2, \text{ for all } (\tau_{l,j}, \tau_{l,k}) \in [0, l_{fj}] \times [0, l_{fk}] \text{ and } \delta T^* \geq \delta T^*_0 > 0 \tag{17}$$

where the desired mission duration is defined as:

$$t^*_d = \int_0^{l_{fj}} \frac{1}{\theta_j(\tau_{l,j})} d\tau_{l,j} = \int_0^{l_{fk}} \frac{1}{\theta_i(\tau_{l,k})} d\tau_{l,k} \text{ for all } j,\ k = 1,\ \ldots,\ n,\ j \neq k, \text{ and } t^*_d \leq T^*_d \tag{18}$$

b. Collision Avoidance in Time

The collision avoidance in time can be achieved by verifying the position of each UAV on a predefined path and, if necessary, by adjusting the discrepancies in position via the speed command of each UAV. The concept of the algorithm is very similar to the one discussed above. The collision can be avoided by not allowing both vehicles to stay in the same space at the same time of the flight. The major difference of this type of collision avoidance is the time constraint, which now means the temporal separation of both vehicles. The framework of collision avoidance in space can be re-used as follows:

$$\min_{j,k=1,\ldots,n,\, j\neq k} \| p_{d,j}(\tau_{l,j}(t_d)) - p_{d,k}(\tau_{l,k}(t_d)) \|^2 \geq E^2, \text{for all } t_d \in [0, t_d^*], \delta T^* \geq \delta T_0^* > 0 \tag{19}$$

Based on the relations (14) – (16), the collision avoidance in time is re-written:

$$\min_{j,k=1,\ldots,n,\, j\neq k} \| p_{d,j}(\tau_{l,j}(t_d)) - p_{d,k}(\tau_{l,k}(t_d)) \|^2 \geq E^2, \text{for all } t_d \in [0, t_d^*], \delta T^* \geq \delta T_0^* > 0, \tag{20}$$

$$t_d^* = \int_0^{l_{fj}} \frac{1}{\theta_j(\tau_{l,j})} d\tau_{l,j} = \int_0^{l_{fk}} \frac{1}{\theta_i(\tau_{l,k})} d\tau_{l,k} \text{ for all } j,\ k = 1,\ \ldots,\ n,\ j \neq k,\ t_d^* \leq T_d^* \tag{21}$$

D. PATH FOLLOWING

The objective of PF is to make the vehicle converge to and follow a desired geometric path; the path can be a solution of either the space or time separation path generation tasks. The control law for PF focuses on the proper control of the pitch and yaw rates, without considering the velocity of the vehicle. It is assumed that the velocity is feasible to sustain the flight. The geometry of the PF problem of a single UAV is presented in Figure 4. The key idea of the PF control algorithm is to use vehicle's attitude control effectors to follow a virtual target vehicle *P* running along the desired path p_d defined in inertial space $\mathcal{I}$.

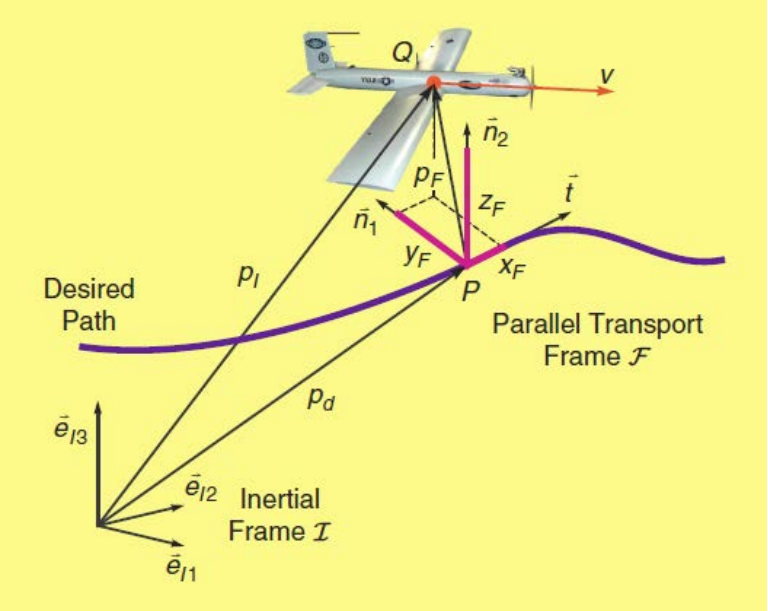

Figure 4. Following a virtual target vehicle.

The problem geometry utilizes two principal coordinate frames, i.e., the inertial frame $\mathcal{I}$ and parallel transport Frame $\mathcal{F}$. Parallel transport frame $\mathcal{F}$ is introduced to define the p_I – position of UAV with respect to the desired position p_d, both expressed in the inertial frame $\mathcal{I}$. The solution of the PF problem is to reduce the PF error p_F to zero by controlling the vehicle's attitude rates; the error is defined as $\overline{p}_F = \overline{p}_I - \overline{p}_d$. The solution of the PF problem for the *i*-th vehicle is independent of the desired speed profile $v_{d,i}$ and uses only local onboard measurement for feedback. The PF control laws represents the outer-loop guidance commands that are to be tracked by the vehicle equipped with an autopilot to ensure the success of the cooperative mission.

Figure 5 demonstrates the geometry of the "cross-track" error p_x, which represents the 3D distance between the actual vehicle *Q* and the virtual target *P*. Figure 5(a) displays the initial p_x when the vehicle is far from the desired path. Figure 5(b) presents a smaller cross track error as the vehicle comes closer to the path. Figure 5(c) presents the situation when the cross track error becomes zero.

The control law that solves the PF problem is given below:

$$\dot{l} = (v\vec{\omega}_1 + k_l p_F)\cdot\vec{t}, \text{ where } k_l \text{ is a positive constant gain.} \tag{22}$$

$$\begin{bmatrix} q_c \\ r_c \end{bmatrix} \triangleq \Pi_R \tilde{R}^{\mathrm{T}} (R_F^D \{\omega_{F/I}\}_F + \{\omega_{D/F}\}_D) - 2K_{\tilde{R}} e_{\tilde{R}} \tag{23}$$

where $K_{\tilde{R}}$ is also a positive feedback gain that drives the PF generalized error vector to a neighborhood of zero (Xargay et al., 2010, p. 59).

The physical meaning of the proposed control law is to drive the distance and the attitude errors to zero by deflecting the control surfaces of lateral and longitudinal channels of a typical airplane.

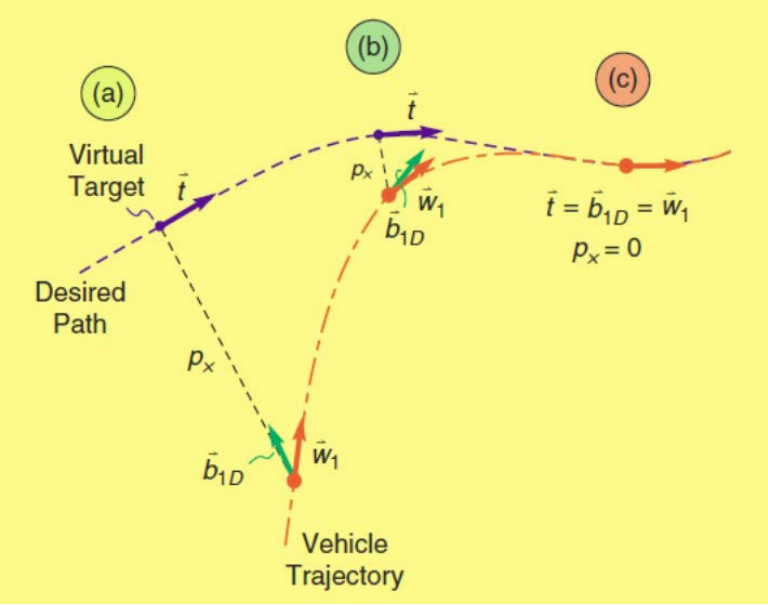

Figure 5. Geometry problem of two-dimensional PF.

E. TIME COORDINATION

The objective of time coordination is to coordinate the pace of progression of multiple autonomous vehicles flying along their corresponding paths. The enabling mechanism (coordination control law) relies on sharing the position on the path over the underlying communication network. The problem of time-critical cooperative path-following control of multiple vehicles is formulated as a classical consensus problem:

the coordination error needs to reach an agreement (converge to the same zero value) on some distributed variables of interest. The coordination variable requires the desired mission duration t_d and the parametric length of the generated path of the *i*-th vehicle $l'_{d,i}(t_d)$. Note that the desired normalized curvilinear abscissa of the *i*-th UAV is defined as:

$$l'_{d,i}(t_d) := \frac{1}{l_{fi}} \int_0^{td} v_{d,i}(\tau) d\tau, \text{ where } v_{d,i} \text{ is the desired speed profile of the } i-\text{th UAV.} \quad (24)$$

The trajectory generation algorithm presented above ensures that the desired speed profile $v_{d,i,}$ satisfy the feasible condition: $0 < v_{\min} \le v_{d,i} \le v_{\max}$, $i = 1, ..., n$, where $v_{\min}$ and $v_{\max}$ denote the minimum and maximum operating speeds of the UAVs in the mission. From equation (20) and the feasible speed condition, it follows that $l'_{d,i}(t_d)$ is a strictly continuous function of t_d mapping $[0, t_d^*]$ on to [0, 1] and satisfying $l'_{d,i}(0) = 0$ and $l'_{d,i}(t_d^*) = 1$. It is also defined $\eta_i : [0,1] \longrightarrow [0, t_d^*]$ to be the inverse function of $l'_{d,i}(t_d)$, $t_d \in [0, t_d^*]$. The normalized curvilinear abscissa at time *t* of the *i*-th virtual target vehicle is re-written.

$$l'_i(t) \triangleq \frac{l_i(t)}{l_{fi}} \quad (25)$$

Then, we define a new time variables:

$$\xi_i(t) \triangleq \eta_i(l'_t(t)), \text{ i=1, ..., n.} \quad (26)$$

If $\xi_i(t) = \xi_j(t) = t'_d$ at a given time t, then $l'_i(t) = l'_{d,i}(t'_d)$ and $l'_j(t) = l'_{d,j}(t'_d)$, which implies that at time *t* the target vehicles corresponding to *i*-th vehicle and *j*-th vehicle have the desired relative position at the desire mission time t'_d

If time derivative $\dot{\xi}_i(t) = 1$, then at time *t*, the *i*-th virtual target travels at the desired speed, $\dot{l}_i(t) = v_{d,i}(\xi_i(t))$. There the variable $\xi_i(t)$ represent the convenient measure of vehicle coordination and are referred to as coordination state, while the functions are called coordination maps. $\eta_i(\cdot)$.

F. COORDINATION LAW

Using the definition of coordination states, we can now define the problem of time-critical cooperative PF for a fleet of *n* UAVs as follow: A fleet of *n* vehicles shares its states on the paths over inter-vehicle communication. While the PF control law requires the pitch and yaw rates for measurements and control, the coordination control law relies on adjusting the speed profile. Thus, the PF error vector converges to zero. Similarly, the coordination errors $(\xi_i(t)-\xi_j(t))$ and $(\xi_i(t)-1)$ converge to neighborhood of the origin.

$p_{d,i}(t_d)$ presents three-dimensional time trajectories, $\zeta_i(t)$ presents *i*-th UAV's status of the coordination, $x_{pf,i}(t)$ presents the PF generalized error vector, and $|\zeta_i(t)-\zeta_j(t)|$ expresses the coordination error between *i*-th vehicle and *j*-th vehicle. Then, *i*-th UAV's coordination state can be defined as follows:

$$\zeta_i(t)=\frac{l_i(t)}{v_{d,i}(\xi_i(t))}, \tag{27}$$

From equation (22), it follows that the evolution of the *i*-th virtual target vehicle along the path is defined as:

$$\dot{l}_i=(v_i\vec{\omega}_{1,i}+K_l p_{F,i})\cdot\vec{t}_i \tag{28}$$

Dynamics of the *i*-th coordination state can be rewritten as:

$$\zeta_i(t)=\frac{(v_i\vec{\omega}_{1,i}+k_l p_{F,i})\cdot\vec{t}_i}{v_{d,i}(\xi_i(t))} \tag{29}$$

Therefore, to solving the equation with respect to velocity defines the command to be sent to the autopilot:

$$v_{c,i}\triangleq\frac{u_{coord,i}v_{d,i}(\xi_i)-K_l p_{F,i}t_i}{\omega_{1,i}t_i}, \tag{30}$$

where $u_{coord,i}$(t) is a coordination control law. The coordination dynamics for the *i*-th target vehicle can be expressed.

$$\xi_i=u_{coord,i}+\frac{e_{v,i}}{v_{d,i}(\xi_i)}\omega_{1,i}t_i, \tag{31}$$

As a result, a decentralized coordination control law can be defined as:

$$u_{coord,1}(t) = -a\sum_{j\in G_1}(\xi_1(t) - \xi_j(t)) + 1, \tag{32}$$

$$u_{coord,i}(t) = -a\sum_{j\in G_1}(\xi_i(t) - \xi_j(t)) + 1 + \chi_{I,i}(t),\ i = 1,\ ...,\ n, \tag{33}$$

$$\chi_{I,i}(t) = -b\sum_{j\in G_1}(\xi_i(t) - \xi_j(t)),\ \chi_{I,i}(0) = 1, i = 2,...,n. \tag{34}$$

G. INFORMATION EXCHANGE ARCHITECTURE

The purpose of this section is to provide the fundamental background knowledge that is required to mathematically describe the concept of information exchange that communicates the coordination states among the vehicles in the same network. Cooperative control strategies for multiple vehicles require exchanging the state information in real time. Communication is critically vital to reduce a risk of midair MAC. In fact, it is impossible to create the perfectly reliable network. For example, there is a probability that the amount of packets on the network happens to be interrupted in the real world. Practical constraints consist of limited bandwidth, unreliable network hardware, limited of fluctuating range of communication, and interruptions. Therefore, the robust network topology of the communication network needs to be carefully reviewed, analyzed, and established.

1. Basic Definition

Graph theory is the foundation of the algorithms developed to enable exchange of information and flight coordination. The communication problem can be modeled with basic primitives that build a graph. A graph is a collection of points called vertices (*V*), which are joined by lines called edges (*E*). When edges have a direction, the graph is called directed. A graph can be expressed in mathematical form, called a matrix. A graph *G* is a pair *(V, E)* where *V* is collection of abstract vertices, written $\{v_1, v_2, \ldots, v_n\}$ and *E* is a collection of ordered pairs of vertices called edges, written $\{e_1, e_2, \ldots, e_n\}$. Let *G* be a graph, then we write *V(G)* to mean the vertex set of *G* and *E(G)* to mean the edge set.

a. Adjacency Matrix

Let *G* be a graph with *n* vertices, $V = \{v_1, v_2, ..., v_n\}$. The adjacency matrix of *G* is the $n \times n$ square matrix $A(G) = (a_{ij})$ defined by

$$a_{ij} = \begin{cases} 1 & \text{if } (v_i,\ v_j) \in E(G) \\ 0 & \text{otherwise} \end{cases} \tag{35}$$

The physical meaning of adjacency matrix is in representing which vertices of a graph are adjacent to which other vertices. In brief, it displays the existence of links around each vertice across the entire network.

b. Degree Matrix

Let *G* be an undirected graph with *n* vertices. The degree matrix of *G*, *D(G)* is the diagonal matrix defined by

$$d_{ij} = \begin{cases} \deg(v_i) \text{ if } i = j \\ 0 \qquad \text{otherwise} \end{cases} \tag{36}$$

As a diagonal matrix, the meaning of this matrix represents the degree of each vertice. For example, the number of communication channels currently opened at a given vertice can be identified by this matrix.

c. Laplacian Matrix

Let *G* be a graph. The Laplacian matrix is a matrix representation of a graph *G*. There are two possible expressions that identically define the same Laplacian: one is defined as $L(G) = D(G) - A(G)$, where *D* is the degree matrix and *A* is adjacency matrix. The other is defined as follows:

$$L = \begin{cases} \deg(v_i) & \text{if } i = j \\ -1 & \text{if } i \neq j \text{ and } v_i \text{ is adjacent to } v_j \\ 0 & \text{otherwise} \end{cases} \tag{37}$$

The physical meaning of the Laplacian represents the state of the network including all nodes and links.

d. Practical Examples

Figure 6 presents a directed graph. Three UAVs communicate with each other according to the following rules: UAV 1 is able to communicate with UAV 2, but, UAV 2 cannot. UAV 1 and UAV 3 can communicate with each other.

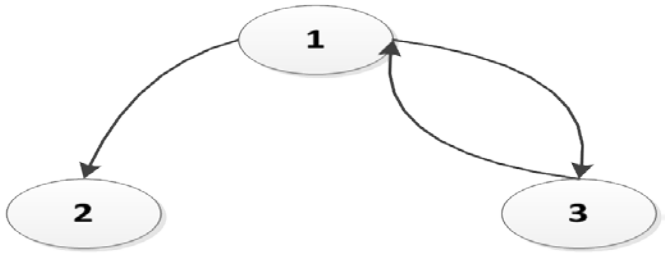

Figure 6. Example topology and the key matrixes. Three elements represent a UAV and the arrow represents the direction of communication.

To express the number of communication channel of the network, the degree matrix can be used and the expression follows:

$$D=\begin{bmatrix} 2 & 0 & 0 \\ 0 & 0 & 0 \\ 0 & 0 & 1 \end{bmatrix} \tag{38}$$

UAV 1 is expressed as d_{11}, which has two communication links. UAV 2 as d_{22} has no communication link with no one. UAV 3, as d_{33} has one communication link.

The adjacency matrix of a graph G, denoted A, is a square matrix with rows and columns indexed by the vertices. Figure 6 identifies three communication links, i.e., one from UAV 1 to UAV 2, another from UAV 1 to UAV 3, and the other from UAV 3 to UAV 1. To express an edge of each UAV, the adjacency matrix is used and can be expressed:

$$A=\begin{bmatrix} 0 & 1 & 1 \\ 0 & 0 & 0 \\ 1 & 0 & 0 \end{bmatrix} \tag{39}$$

The Laplacian matrix is a simplest mathematical expression of graph *G*, presenting the number of nodes and the value of link at the same time. The Laplacian matrix of Figure 6 is expressed as follows:

$$L = D - A = \begin{bmatrix} 2 & -1 & -1 \\ 0 & 0 & 0 \\ -1 & 0 & 1 \end{bmatrix} \tag{40}$$

e. The Consensus Dynamic

In addition, the Laplacian matrix is directly applied in the consensus dynamic. A general matrix representation of the consensus algorithm is expressed as:

$$\dot{x}(t) = -L(t)x(t) \tag{41}$$

where $x = [x_1, x_2, \ldots, x_n]^T$ is the information state, and $L(t) = [l_{ij}(t)] \in R^{n \times n}$ is the Laplacian of the underlying communication graph.

For example, the consensus problem expressed by equation (41) in application to the communication topology example presented in Figure 6 results in the following expression:

$$L\xi = \begin{bmatrix} 2 & -1 & -1 \\ 0 & 0 & 0 \\ -1 & 0 & 1 \end{bmatrix} \begin{bmatrix} \xi_1 \\ \xi_2 \\ \xi_3 \end{bmatrix} = \begin{bmatrix} 2\xi_1 - \xi_2 - \xi_3 \\ 0 + 0 + 0 \\ -\xi_1 + \xi_3 \end{bmatrix}, \tag{42}$$

where ξ is the state information communicated over the network by vehicle *i*.

Observe, that each element of resulting $L\xi$ equation represents naturally the coordination errors. Therefore, if the coordination dynamics defined by the vector differential equation (41) converges to a stable solution, then all coordination errors arrive to zero. That is the objective of the coordination algorithm.

As a result, a decentralized network topology and the consensus task defined over the time varying network can be conveniently represented and solved by the tools defined in algebraic topology. Therefore, the communication of coordination states among a shared inter-vehicle network can be feasible for real-time, onboard implementation, thus providing a viable practical solution.

2. Consensus Algorithm

Ren et al. (2007) states that information consensus guarantees that vehicles sharing information over a noisy time-varying network topology have a consistent view of information that is critical to coordination tasks. Consensus algorithms are designed to be distributed, assuming that only neighbor-to-neighbor interaction between vehicles is available. Each vehicle updates its own information state, based on the information states of its neighbor. Extending the consensus algorithm to multiple vehicles and expressing the vector equation (41) in scalar form results in the following intuitive form.

$$\dot{x}_i(t) = -\sum_{j=1}^{n} a_{jk}(t)(x_i(t) - x_j(t)),\ i = 1,\ ...,\ n, \tag{43}$$

where $a_{ij}(t)$ is the (i, j) entry of the adjacency matrix of the associated communication graph at the time t, and x_i is the information state (in our case, it is the relative position of a UAV on the path) of the i-th vehicle.

When state information is exchanged between vehicles through a communication network, the time delay associated with both the message transmission and processing after receipt must be considered. In an asynchronous consensus framework, each vehicle exchanges information asynchronously and updates its own state, which possibly is based on outdated information from its local neighbors. As a result, heterogeneous agents, time-varying communicate delays, and packet dropout must all be taken into account in the same asynchronous consensus framework. The equation (43) can be re-written as:

$$\dot{x}_i(t) = -\sum_{j=1}^{n} a_{jk}(t)[x_j(t - \sigma_{ij}) - x_i(t - \sigma_{ij})], \tag{44}$$

where σ_{ij} is the time delay between i-th and j-th vehicle; and $\sigma_{ij} = \sigma$ and the communication topology is fixed, undirected, and connected, average consensus is achieved if and only if $0 \le \sigma_{ij} < (\pi / 2\lambda_{\max}(L))$, where L is the Laplacian of the communication graph.

3. Coordination Control Law

The coordination laws that are based on the state information exchange among vehicles in time varying networks are expressed next in the equations (32), (33), and (34).

The 1st vehicle is elected as the formation leader. A constant value *a* and *b* is a positive adjustable gain. The coordination state error between *i*-th and *j*-th vehicle is expressed as $|\xi_i(t)-\xi_j(t)|$, and the coordination error $\chi_{I,i}(t)$ between two vehicles is defined in (34). The coordination law consists of three parts, such as coordination of the formation leader, coordination of the *i*-th vehicle and coordination error between vehicles in real time. The control law follows:

$$u_{coord,1}(t) = -a\sum_{j\in G_1}(\xi_1(t)-\xi_j(t))+1 \tag{32}$$

$$u_{coord,i}(t) = -a\sum_{j\in G_1}(\xi_i(t)-\xi_j(t))+1+\chi_{I,i}(t),\ i=1,\ ...n, \tag{33}$$

$$\chi_{I,i}(t) = -b\sum_{j\in G_1}(\xi_i(t)-\xi_j(t)),\ \chi_{I,i}(0)=1, i=2,...,n, \tag{34}$$

H. SPACE AND TIME SEPARATION EXAMPLE

Upon complete implementation of all required algorithms above, the following results present the examples of successful collision avoidance in time and space.

1. Example of Collision Avoidance in Time

Figure 7 illustrates the solution of the CPF task. The objectives are to maintain a desired spatial clearance minimum of 500 meters, to complete the mission within the desired mission duration of 160 seconds, to avoid collision in time, and to depart and arrive at the defined locations.

Figure 7(a) demonstrates the simulation result of the collision avoidance in time algorithm while UAVs are flying along the 3D spatial paths. The bar between path 1 and path 2 is identified as the required distance threshold. Figure 7(b) demonstrates the speed profile of both vehicles with the maximum and minimum speed boundaries. Figure 7(c) demonstrates the path separation in 3D. Figure 7(d) demonstrates the magnitude of vehicle separation.

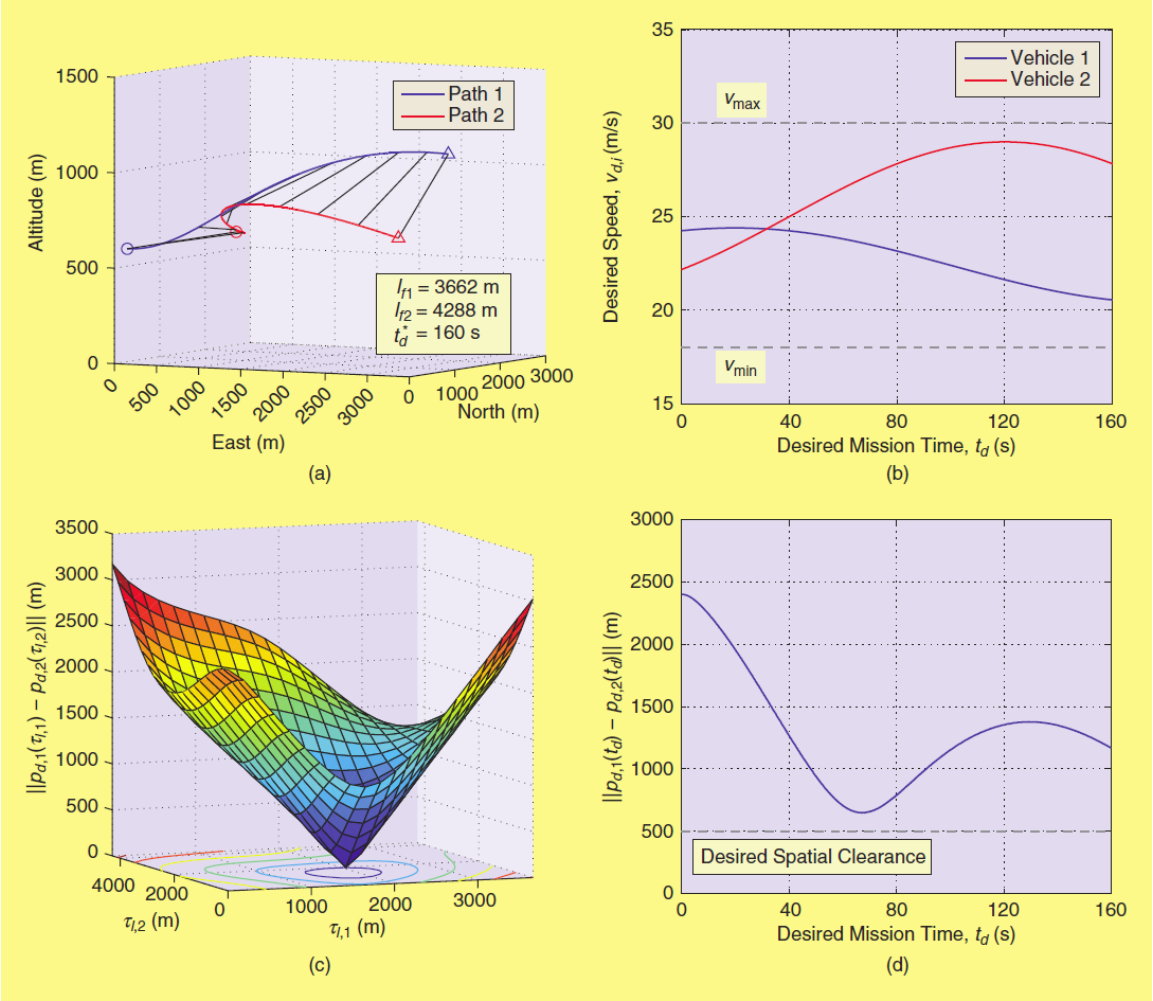

Figure 7. Collision avoidance in time with two UAVs adapted from "Time-Critical Cooperative Control of Multiple Autonomous Vehicles," by Xargay et al., 2010. (a) Three-dimensional spatial paths, (b) Speed profiles, (c) Path separation, (d) Vehicle separation.

2. Example of Collision Avoidance in Space

Figure 8 illustrates another case of the CPF task. The objectives are to maintain no feasible path intersection, to complete the mission within the desired mission duration of 160 seconds, to avoid collision by collision avoidance in space algorithm, and to depart and arrive at the planned location while maintaining the distance threshold. The algorithm requires no path intersection of both vehicles during the entire CPF task.

Figure 8(a) demonstrates the simulation result of the collision avoidance in time algorithm while UAVs are flying along 3D spatial paths. Figure 8(b) demonstrates the

speed profile of both vehicles within maximum and minimum speed boundaries. Both vehicles demonstrate a mild speed change during the flight. Figure 8(c) demonstrates the path separation in 3D. Figure 8(d) demonstrates the 3D vehicle separation.

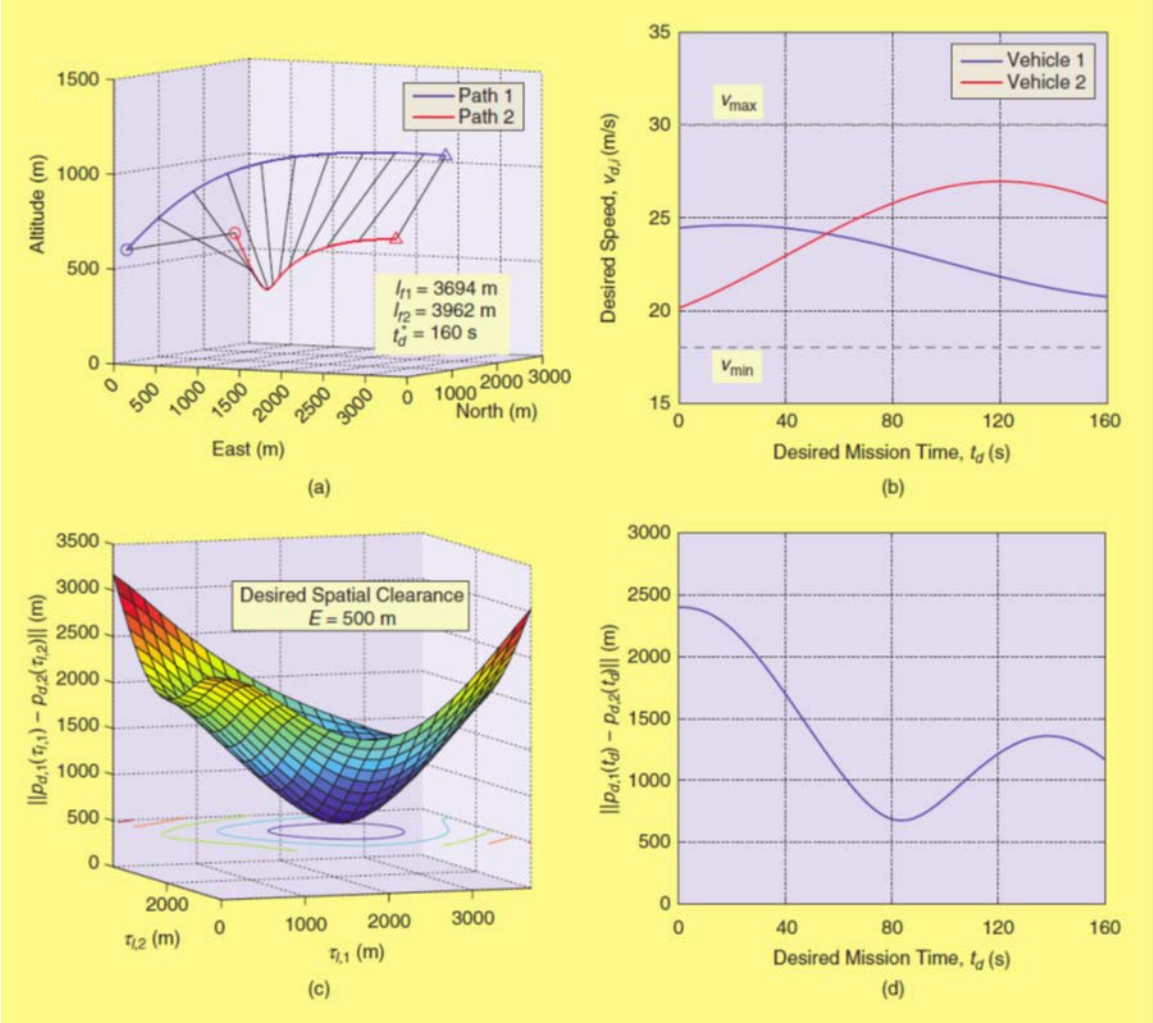

Figure 8. Collision avoidance in space with two UAVs adapted from "Time-Critical Cooperative Control of Multiple Autonomous Vehicles," by Xargay et al., 2010. (a) Three-dimensional spatial paths, (b) Speed profiles, (c) Path separation, (d) Vehicle separation.

III. IMPLEMENTATION OF THE COORDINATED PATH FOLLOWING

The primary objective of the chapter is to describe the implementation of the mathematical models of previously discussed algorithms in Mathworks Simulink®. Mathworks Simulink® is a block diagram environment for multi-domain mathematical modeling and simulation. It allows building, simulating, and analyzing the mathematical models of various real-time dynamic processes. This chapter develops numerical models of each algorithm demonstrated in Chapter II, such as PF, time coordination, and communication, and addresses the fundamental functionality of each algorithm.

A. DIAGRAM OVERVIEW

The mathematical model of CPF capability consists of five major components, including the six Degree of Freedom (DOF) Equations of Motion (EOM) model, the PF controller, the coordination controller, and the communication controller. Figure 9 displays the top-level view of the CPF model of two UAVs. On the diagram, both UAV models and their corresponding CPF controllers are algorithmically identical.

The UAV model consists of the 6 DOF-EOM model of a generic fixed-wing airplane equipped with a stabilizing autopilot. The PF module enables the vehicle to perform an assigned mission by generating a path, following the path, and exchanging the state information in real time, which, in turn, enables coordination. The first primary element in the control parameters' block is a path generator, which produces a path based on the assigned mission criteria, initial and final conditions, and operational constraints. The path generator requires information about the boundary conditions of each airplane, including the initial and the final three-dimensional position of each UAV, and the magnitude and orientation of their velocity vectors. At the output, the algorithm produces a 3D path for each of the UAVs. The "Graphical Output" subsystem is responsible for displaying the graphical output of the simulation results in the 3D coordinate frame.

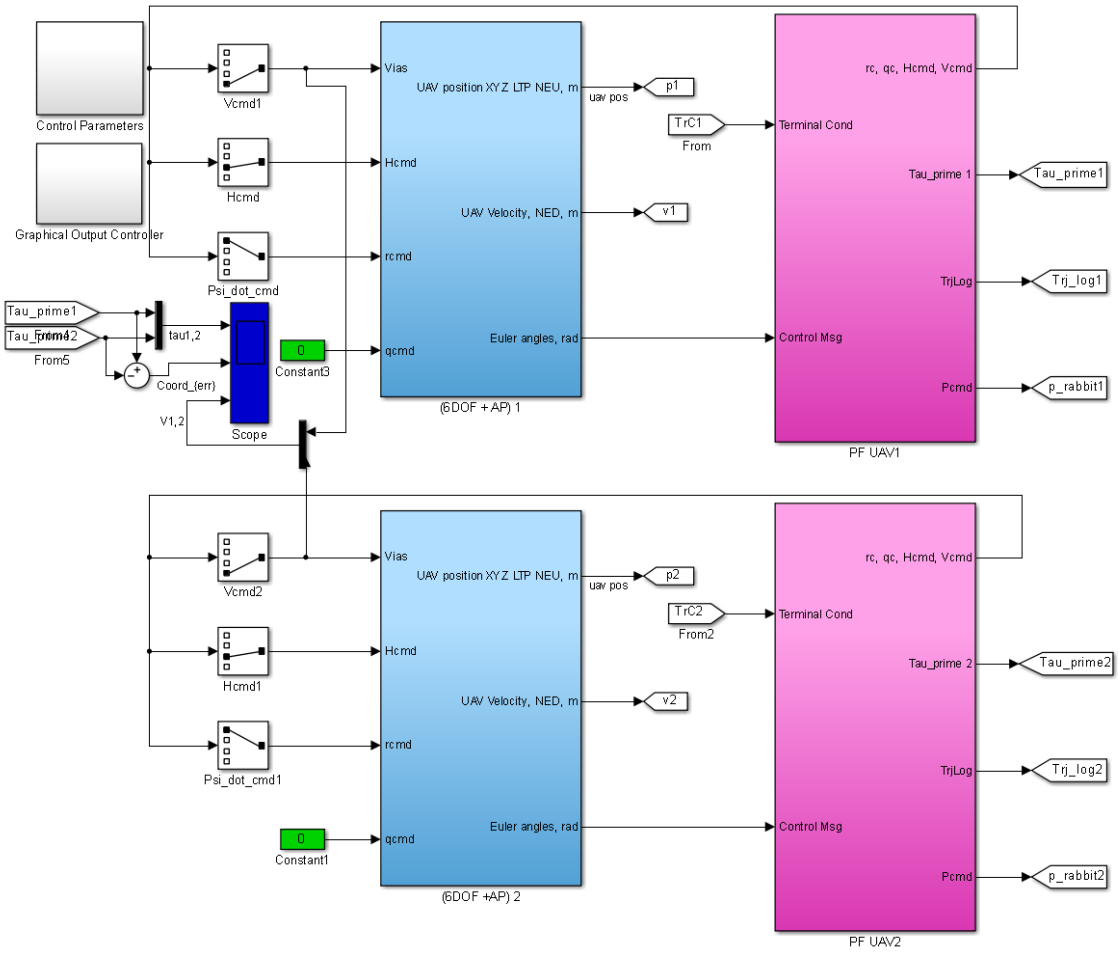

Figure 9. CPF Model of two UAVs. The diagram demonstrates the top-level architecture of the model.

B. UAV AND AUTOPILOT

Figure 10 illustrates the 6 DOF-EOM model of UAV equipped with an autopilot. The primary function of the autopilot consists of stabilizing the airplane's dynamics. The Piccolo autopilot is used as a prototype. It enables a UAV to perform its mission without human interruption, and is capable of processing a complete set of inertial, GPS and barometric measurements, thus producing the flight stabilization commands for the control surfaces. The Piccolo autopilot and the 6 DOF-EOM models establish a plant that is being controlled by the PF controller.

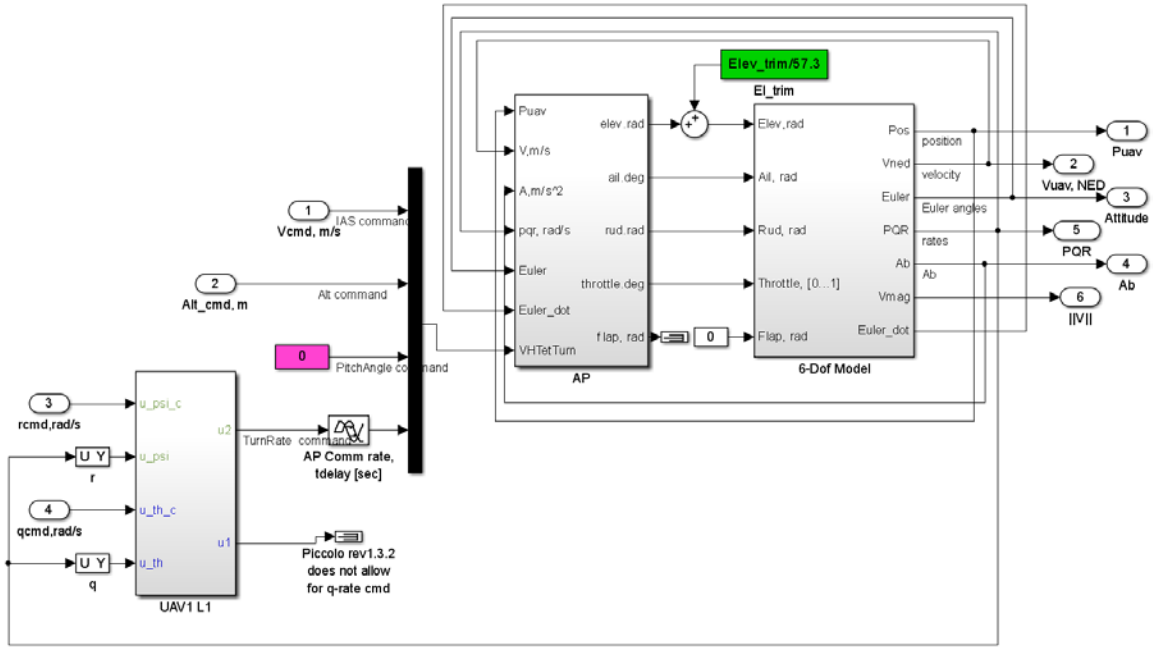

Figure 10. The UAV with autopilot Module. The module consists of autopilot and the 6 DOF-EOM modules.

C. PATH FOLLOWING CONTROLLER

The purpose of the module is to control the vehicle kinematics by means of PF commands. Figure 11 consists of the “Computing PF Errors” and the “Computing PF Commands” models. The “Computing PF Errors” model computes the current errors of a UAV with respect to the desired path calculated by the path generation algorithm. The “Computing PF Commands” model calculates the control commands required to drive the PF errors to zero.

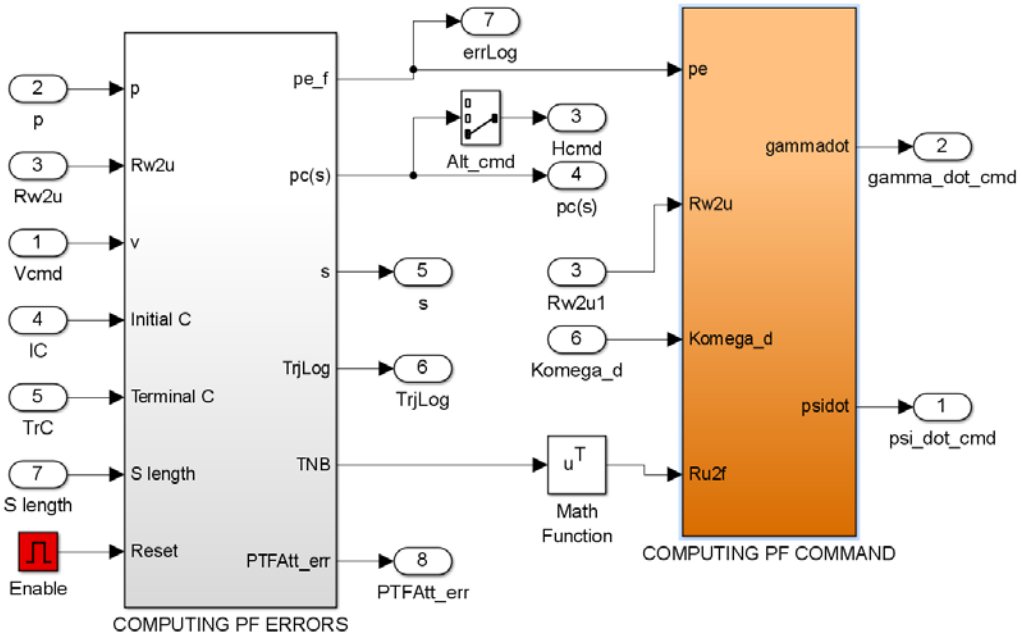

Figure 11. The CPF Controller.

D. COORDINATION CONTROLLER

1. Implementation of Consensus Algorithm

Figure 12 illustrates the Simulink implementation of the mathematical idea of the consensus algorithm; for the sake of clarity the figure details the structure of the controller and uses the Laplacian of the communication topology previously defined in Figure 6. The diagram consists of the Laplacian matrix representing the current communication topology as an input, the consensus model defined in equation (41) and the Proportional Integral (PI) controller. The Laplacian matrix defines the instantaneous topology of communication networks. It is implemented as matrix *L*. The Laplacian in Figure 12 presents the network topology, previously discussed in Chapter II; see Figure 6. The consensus algorithm model is initialized with the initial conditions, such as 10 meters, 50 meters, and 100 meters; the conditions define the state of coordination variable (relative position on the path) at the beginning of simulation. The objective of the PI controller is to drive the coordination errors to zero; the importance of the PI controller is justified in the next section.

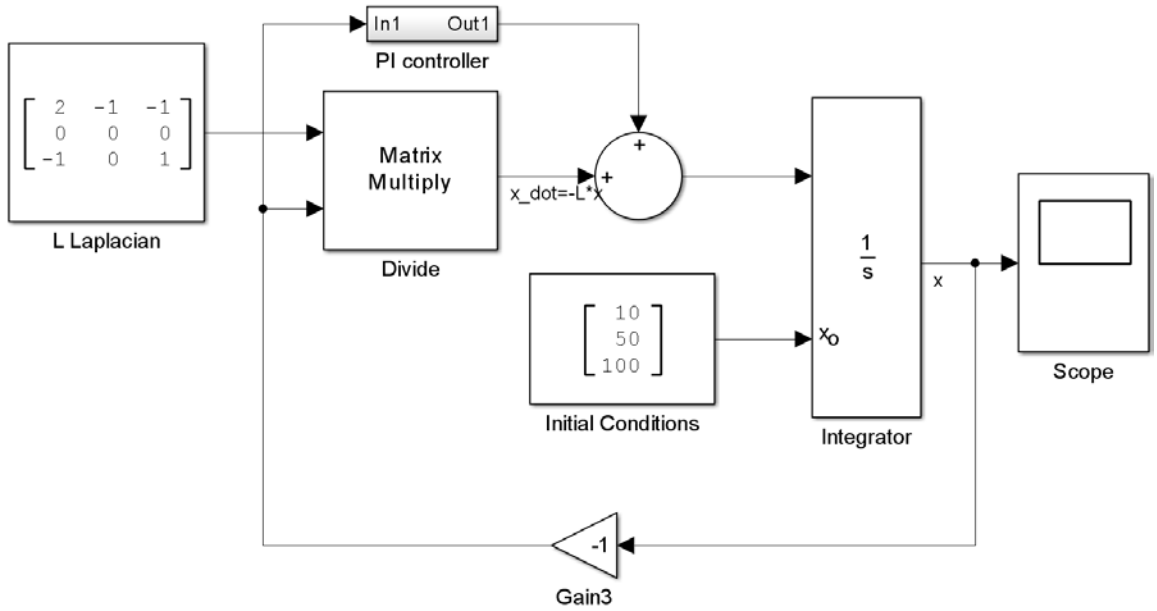

Figure 12. Practical implementation of consensus algorithm, discussed in Figure 6.

a. Simulation Result of the Consensus Algorithm without the PI Controller

Figure 13 demonstrates the importance of the PI controller. First, consider the case when there is no controller implemented around the given coordination architecture. The markers at time zero indicate the initial conditions of all UAVs: red line with the circle marker indicates UAV 1 at 10 meters at time zero, the blue line with the diamond marker indicates UAV 2 at 50 meters at time zero, and the brown line with the rectangular maker indicates UAV 3 at 100 meters at time zero. Since UAV 2 has no communication ability, it cannot produce any coordination commands and cannot respond to any commands from the neighbors. UAV 1 and UAV 3 coordinate their states into the median value. As a result, the integrated controller fails to zero the coordination errors; the final states converge to a median value instead of zero.

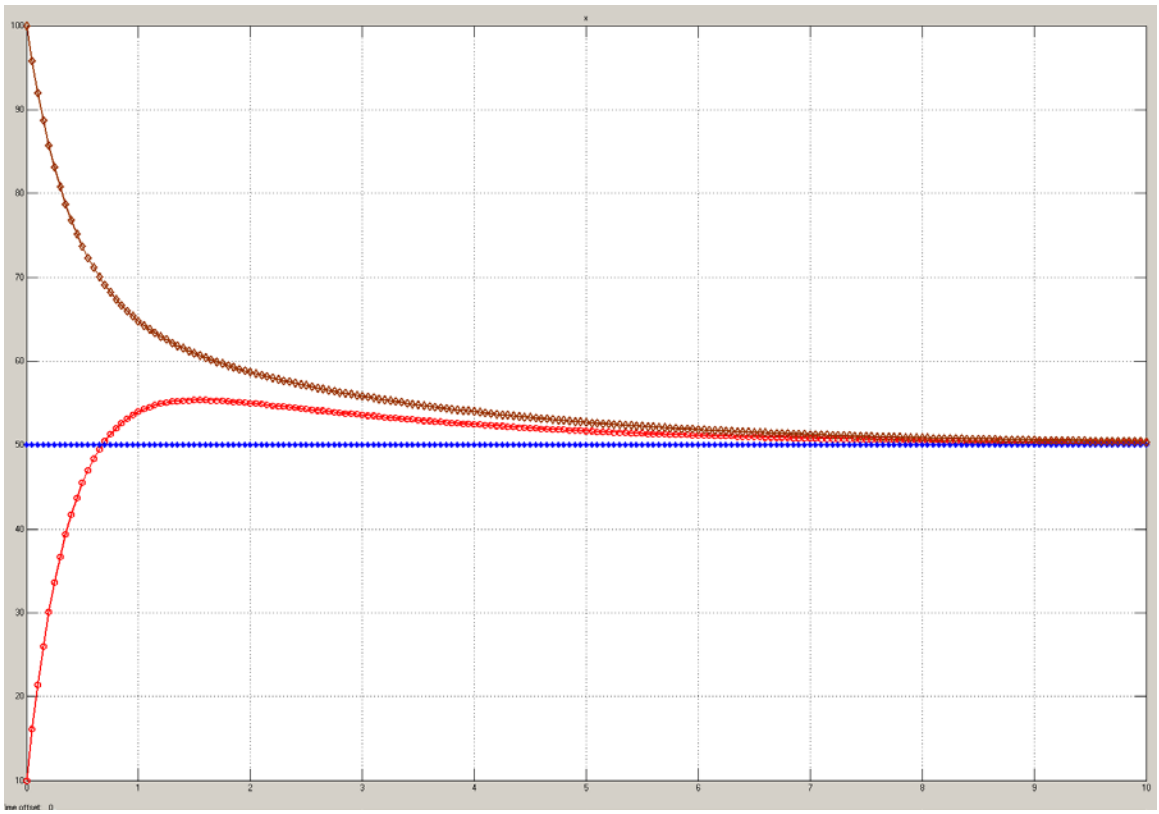

Figure 13. The simulation result of the consensus algorithm without the PI controller. The initial condition is assigned at 10m, 50m, and 100m. The final states converge to a median value instead of zero.

b. Simulation Result of the Consensus Algorithm with the PI Controller

The goal of consensus algorithm in the CPF task is to eliminate the errors in coordination states and to drive them all to zero. To achieve the zero coordination errors, consider a modification of the coordination dynamics where the same architecture is augmented with the PI controller. Figure 13 demonstrates the dynamics of coordination states in this new case. It can be observed that the PI controller removes an adverse bias and drives all coordination errors to zero in approximately 0.5 second.

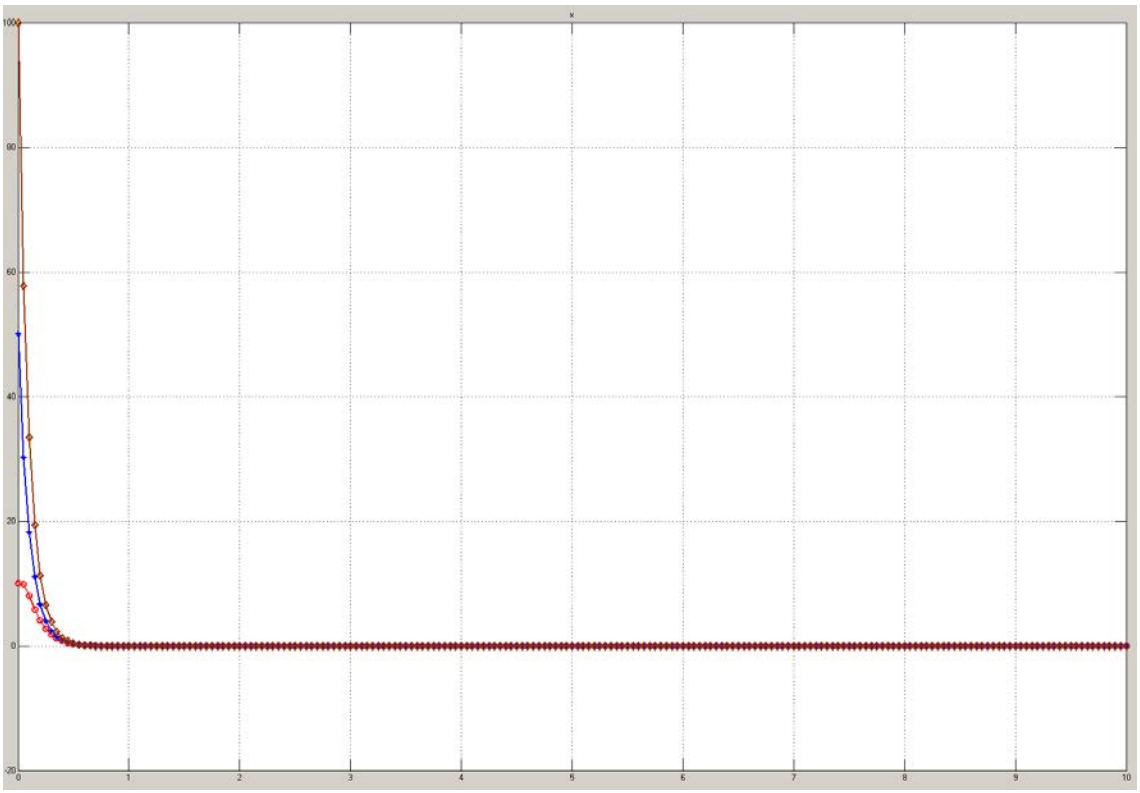

Figure 14. The simulation result of the consensus algorithm with the PI controller. The initial condition is assigned at 10m, 50m, and 100m. The coordination is achieved in approximately 0.5 second.

2. Coordination Controller

Figure 15 demonstrates the flight test implementation of coordination control law, defined in equation (32) – (34). The coordination model includes the speed adjustment law, the Laplacian input, which is the matrix representation of the information exchange network, and the current position calculator block. The "Current Position calculator" block receives two inputs (since we work with two UAVs), the current position and the total mission length of own UAV, and returns a normalized value of the state. The output of the UAV's own state and the state of the other vehicles become the input of the speed coordination controller. The speed coordination controller processes the state of communication network condition captured by the Laplacian of both vehicles and provides a velocity adjustment. The key concept of this decentralized coordination is to share the UAV's own state with the other UAVs on the same network and to adjust the UAV's own relative position by modifying the velocity command. All other UAVs

possess the same coordination controller and modify their own states based on the exchange of state information. The nature of this coordination is distributed in a way that is extremely beneficial in a networked system.

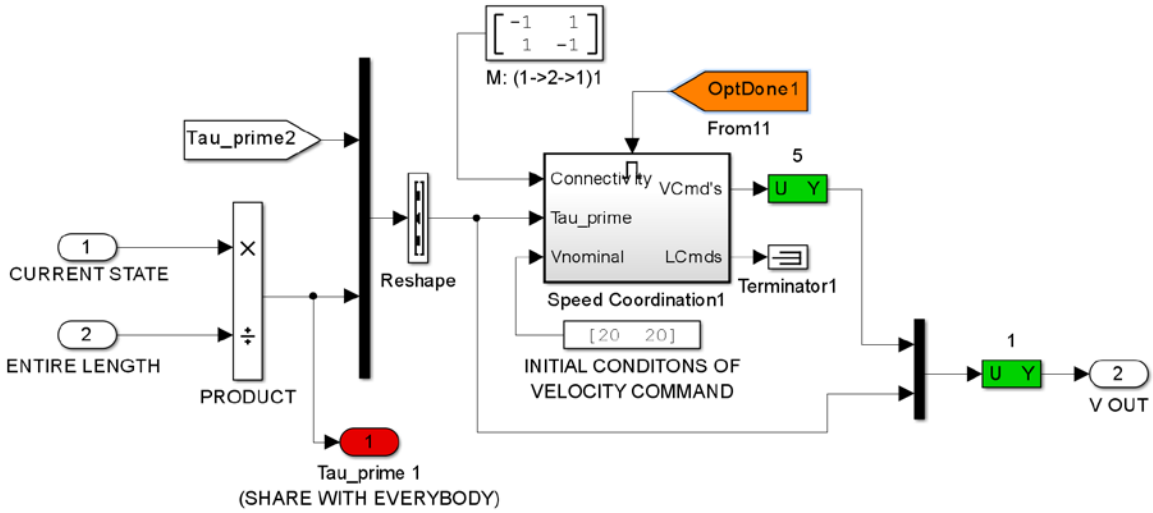

Figure 15. Simulink diagram that implements the time critical cooperative coordination control law.

IV. EXPERIMENTAL RESULTS

The objective of this chapter is to evaluate the impact of intermittent loss of communication among multiple UAVs on the performance of coordination expressed in terms of coordination states error and the Euclidian distance between vehicles. As discussed in the previous chapters, the coordination among multiple UAVs is the method of keeping them safely separated in 3D space, which is the proposed approach achieved by exchanging a single relative position parameter among the vehicles in the fleet. This is in high contrast with the more expensive methods currently used to transmit an extensive number of parameters.

This chapter is in fact a comparative study. The objective of this study is achieved by implementing the numerical models of six-DOF dynamics of UAVs, the PF and coordination algorithms communicating across the time-varying network in MatLab/Simulink environment. The chapter starts with an introduction of the nominal scenario where two identical UAVs are set to cross paths once by following two ideally symmetric trajectories while flying under perfect communication conditions. This setup allows establishing the *baseline performance* of time coordination. This step illustrates that under ideal conditions both UAVs will necessarily collide; therefore, a need for biasing (offsetting) the coordination states is established. With this trivial modification, the same set of algorithms is then used to illustrate the biased coordination of two UAVs resulting in perfect collision avoidance that satisfies the 3D separation assurance threshold. At the next step, the performance of coordination of UAVs while following the paths is varied by introducing the variable *periods of no communication*. The impact of degraded communication is analyzed in terms of the Euclidian separation and the variation of coordination parameter. The chapter ends with the analysis of the numerical results and conclusions, thus highlighting the performance of the proposed approach.

A. DESIGN OF THE EXPERIMENT

First, we need to describe the simulation conditions that are used throughout the entire chapter. To illustrate the performance of time-critical coordination, it is necessary

to isolate all factors that might distort and interrupt the simulation results by adversely affecting the coordination abilities of UAVs. Among these factors, there might be an unequal length or different shape of the paths assigned to the UAVs, or different flight dynamics characteristics of the vehicle. Although they might be valuable factors to consider, at the initial stage when the baseline performance is of interest, they must be excluded.

To achieve this goal, a set of symmetric flat (2D) trajectories is designed by assigning symmetric boundary conditions and identical length of the paths for two UAVs. The boundary conditions that include initial (IC) and final conditions (FC) are chosen because the paths have a single point of intersection and they are placed sufficiently far from the starting location of the numerical simulation. A sufficiently distant collision point is necessary to account for the initial transients that the UAVs might experience at the beginning of their flight; the transient can be associated with various real-life factors including, for example, some imperfections in numerical simulation of the UAV dynamics. Moreover, at this step, the simulation will assume ideal communication conditions; therefore, no communication loss will be introduced. This assumption results in UAVs following their paths with the coordination control law not affected by any feedback delays in measuring the relative position of vehicles.

1. Simulation Setup

The parameters of symmetric simulation are presented next in Table 3. Note that the path parameterization results in the initial position of each UAV to correspond to $\xi_i^{IC} = 0$ and the final position to correspond to $\xi_i^{FC} = 1$ of the coordination state

Boundary Condition	Parameter	Value
	simulation time	255, sec
	relative length of the paths	450, dimensionless
IC of UAV1	initial position of UAV 1 in NEU	[0 150 700], m
	initial body velocity of UAV 1	22, m/s
	initial Euler angles of UAV 1	[0 0 -45], deg
FC of UAV1	final position of UAV 1 in NEU	[5000 -150 700], m
	final body velocity of UAV 1	23, m/s
	final Euler angles of UAV 1	[0 0 -45], deg
IC of UAV2	initial position of UAV 2 in NEU	[0 -150 700], m
	initial body velocity of UAV 2	22, m/s
	initial Euler angles of UAV 2	[0 0 45], deg
FC of UAV2	final position of UAV 2 in NEU	[5000 150 700], m
	final body velocity of UAV 2	23, m/s
	final Euler angles of UAV 2	[0 0 45], deg

Table 3. Parameters of the symmetric simulation.

Next, the condition of lossless communication is implemented in the numerical simulation of two UAVs assigned to follow the resulting symmetric trajectories with ideal coordination. The resulting generated paths and the actual paths of both UAVs are presented in Figure 16. Both generated (desired) paths are identified by the dotted lines. In turn, the actual paths of both UAVs are drawn in the solid lines—red line for UAV1 and blue line for UAV 2. First, the simulation illustrates the symmetry of the setup and highlights the fact that under ideal communication conditions, both UAVs will necessarily collide; flying at the same altitude along the symmetric trajectories results in the collision around the 112.56 seconds of flight. Second, it is clear that under nominal flight conditions (no excessive wind and other flight dynamics related disturbances) it is possible to separate the PF from coordination. This is a significant benefit of the entire CPF approach, which in turn enables separate analysis of the coordination performance.

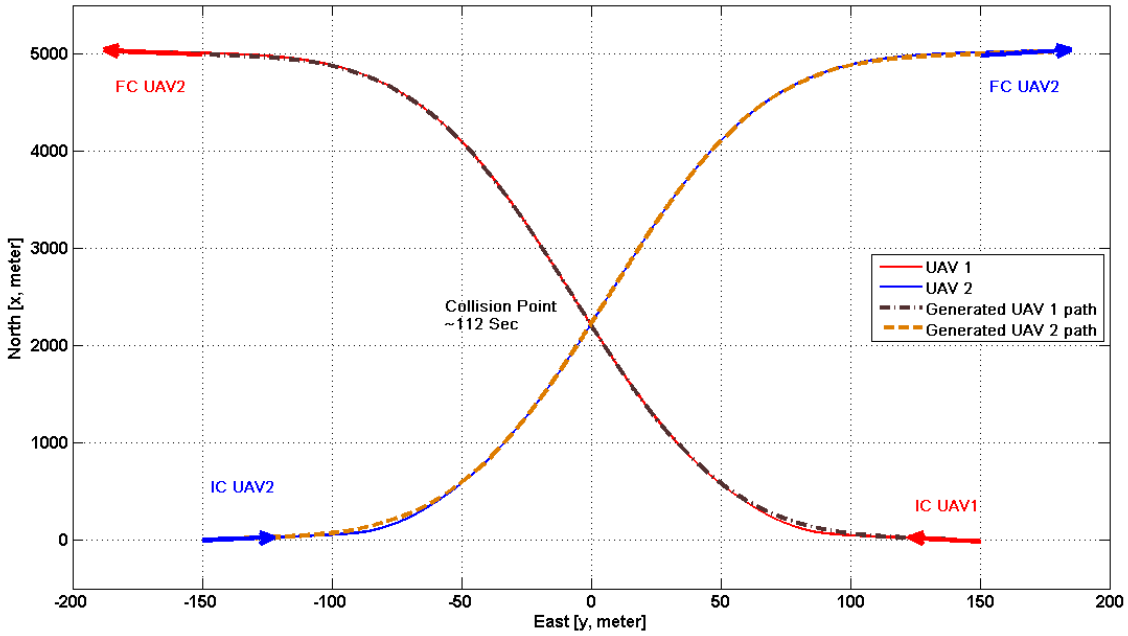

Figure 16. Results of simulating 2 UAVs following symmetric paths. Note that the scales along the axis are not the same.

The performance of coordination in the simplified scenario is characterized by the difference in coordination states ξ_i that are controlled onboard each vehicle so that all states ξ_i across the fleet of UAVs achieve the same value and progress with the same pace. Figure 17 illustrates the dynamics of coordination states ξ_i , their difference $\xi_1 - \xi_2$, the control efforts resulting from the objective of coordination, and the Euclidian distance between two UAVs. The control efforts are presented here in terms of the commanded air speed $V_{cmd,\,i}$ that is a typical control parameter for majority of modern UAVs. Subplots 1 and 2 demonstrate the ideal coordinated states of both UAVs; the states are practically the same along the entire flight and the separation between them, which is caused by the minor flight dynamics difference, is kept near zero all the time. This result is predictable because there is no communication loss. The third subplot presents the velocity profiles of both UAVs; the plot includes both the commanded velocities $V_{cmd,\,i}$ and actual velocities $V_{act,\,i}$ of each UAV. The final subplot 4 demonstrates the Euclidian separation distance between the UAVs. As expected, since both UAVs hold

the same altitude of 700 meters and coordinate perfectly, there is only one collision point that occurs at 112.56 seconds.

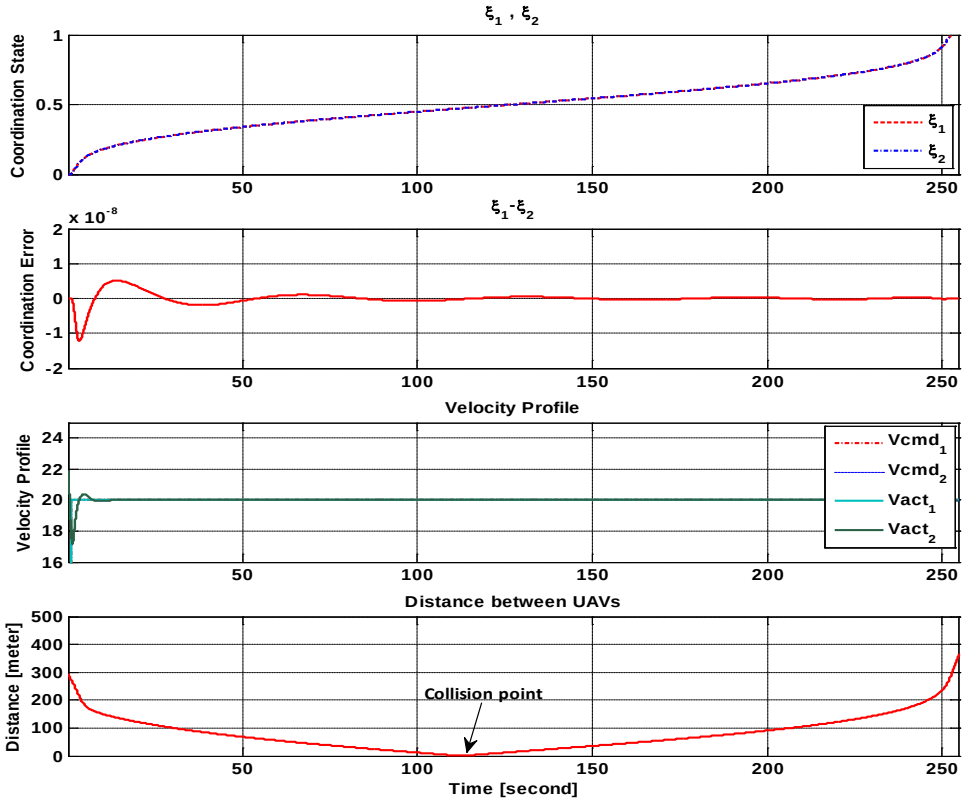

Figure 17. Coordination parameters in symmetric setup under lossless communication conditions.

An obvious conclusion that can be drawn from this simulation is that the perfect solution of the coordination problem results in a MAC while the goal of the thesis is to guarantee a collision-free flight. The solution to this problem is to consider the following question: What can be done to separate the UAVs in flight, assuming that each UAV has a method of achieving perfect coordination of its state ξ_i with another nearby flying UAV? The trivial solution is to exploit this perfect coordination capability by requiring each UAV to follow, not a zero coordination error, but a fixed non-zero reference that should reflect D_E the desired 3D separation in space ($\xi_1 - \xi_2 = \delta(D_E) = const$).

Therefore, introducing a reference $\delta(D_E)$ into the coordination algorithm will be considered next as a solution of the collision avoidance problem. The relation between the dimensionless $\delta(D_E)$ and physical separation D_E measured in the units of length in application to the considered symmetric case is as follows:

$$D_E = L \cdot \delta_E , \tag{45}$$

where L is the normalized total length of the path used at the path generation phase.

2. Ideal Communication Condition with Non-Zero Coordination Reference

First, it is still necessary to obtain the nominal performance of the coordination algorithm under ideal communication conditions for the case of non-zero coordination reference. Before proceeding to the simulation, it is necessary to design a simple algorithm for introducing this reference. The solution should be mathematically general and technically sound so that both cases of zero and any arbitrarily chosen reference can be easily implemented.

Consider equation (41) in Chapter II, which describes the basics of the consensus problem ("arrive to the same state across the networked nodes"), where the L – is Laplacian matrix. In the conditions of perfect communication (lossless) and no communication (100% of communication loss) it can be defined as follows:

$$0\%\ \text{Loss: } L = \begin{pmatrix} 1 & -1 \\ -1 & 1 \end{pmatrix}, \tag{46}$$

$$100\%\ \text{loss: } L = \begin{pmatrix} 0 & 0 \\ 0 & 0 \end{pmatrix}, \tag{47}$$

When the coordination is achieved, the states of both UAVs converge to the same value ($\xi_1 = \xi_2$) resulting in the pace of change of states to be zero ($\dot{\xi}_1 = \dot{\xi}_2 = 0$), thus not requiring any control efforts. Mathematically this idea is described by the following differential equation (assume no communication loss):

$$\dot{\overline{\xi}} = -L\overline{\xi} = \begin{pmatrix} \dot{\xi}_1 \\ \dot{\xi}_2 \end{pmatrix} = -\begin{pmatrix} 1 & -1 \\ -1 & 1 \end{pmatrix}\begin{pmatrix} \xi_1 \\ \xi_2 \end{pmatrix} = -\begin{pmatrix} \xi_1 - \xi_2 \\ \xi_2 - \xi_1 \end{pmatrix} => \begin{pmatrix} 0 \\ 0 \end{pmatrix} \tag{48}$$

Now it becomes clear that introducing a non-zero reference can achieve the same coordination goal with the following simple modification:

$$\dot{\bar{\xi}} = L(\bar{\xi} + \bar{\delta}) = \begin{pmatrix} 1 & -1 \\ -1 & 1 \end{pmatrix} \left[\begin{pmatrix} \xi_1 \\ \xi_2 \end{pmatrix} + \begin{pmatrix} -0.02 \\ 0.02 \end{pmatrix} \right] , \tag{49}$$

where ±0.02 is chosen to enforce the UAV 2 to be behind the UAV 1 by this non-zero coordination reference. This approach is universal because if perfectly synchronized coordination is required then the value of $\bar{\delta}$ vector can be easily changed to $\bar{0}$. The Simulink implementation of the non-zero coordination reference algorithm is illustrated next in Figure 18.

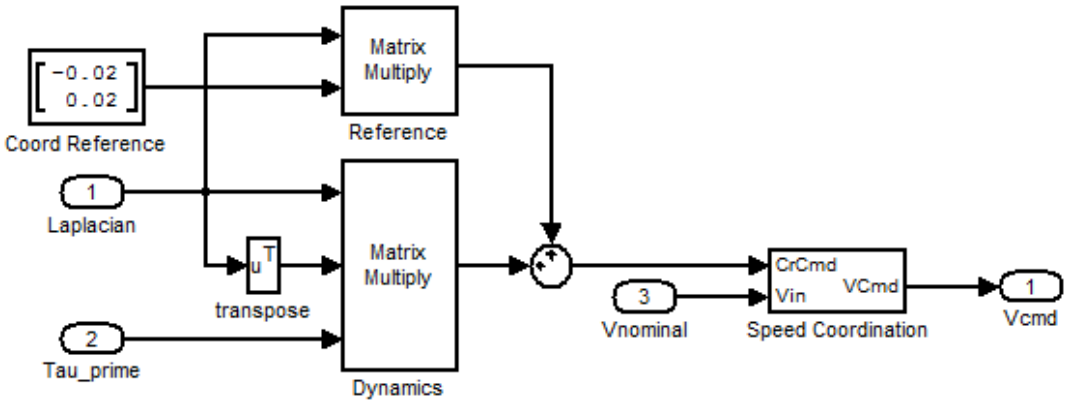

Figure 18. Simulink implementation of non-zero coordination reference.

Figure 19 illustrates the result of simulation for the considered case; both UAVs are assigned to follow previously designed symmetric paths in the conditions of no communication loss. The content of the figure is identical to Figure 17. Analysis of the result shows that, although both UAVs stay on the same paths, the collision is avoided by slowing UAV 2 and speeding up UAV 1 (see the separation distance subplot). Since both UAVs start at the $\xi_i = 0$ there is an initial coordination error (with respect to the desired reference) and transient that separates the coordination states and settles at the required reference value. The coordination is achieved by adjusting the commanded speed of UAVs. It is clear that each UAV has an internal non-trivial (there is no an immediate response) dynamics in the speed channel; this is illustrated by the fact that the actual

speed of each UAV is lagged behind the commanded airspeed. The Euclidian separation distance plot explicitly shows that there is no collision and allows establishing the separation bound $D_E = 150, m$ to be used in further comparison study.

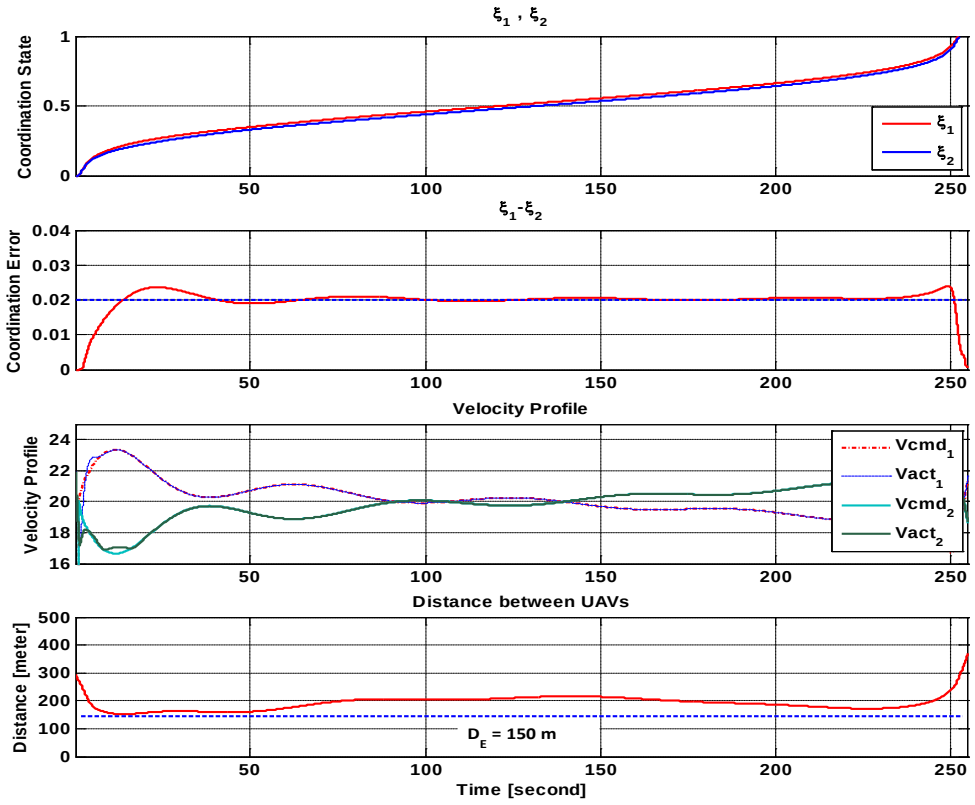

Figure 19. Result of coordination under ideal communication and non-zero coordination reference.

3. Variation of the Communication Conditions

This section evaluates the influence of communication loss on the coordination performance during the simulated flight. By varying the interval of "no communication" with respect to the "nominal duration of the communication frame," it is possible to conveniently model the loss of information. The duration of the "nominal communication frame" is chosen to be significantly longer then the lag time associated with the speed dynamics of UAVs. Based on the observation of the real speed dynamics characteristics

of Rascal UAV operated by NPS, the duration of the "nominal communication frame" was chosen to be 10 sec. To conveniently model the time-varying communication topology and introduce variable communication period, a simple model of "switch" has been developed and implemented in Simulink; see Figure 20.

Pulse Generator	The communication scheduler
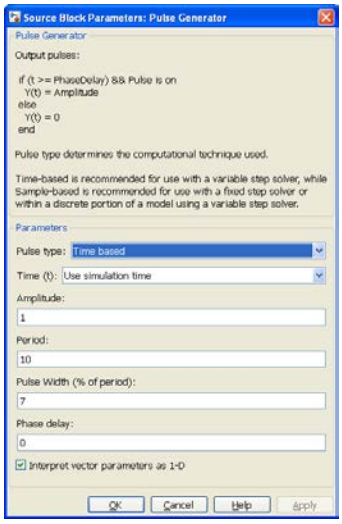	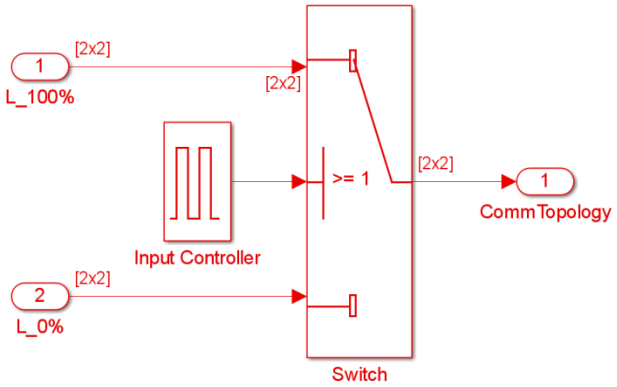

Figure 20. Simulink implementation of the loss of communication scheduler.

The algorithm utilizes the pulse signal to switch between two communication topologies (100% and 0% communication). Varying the pulse width of a standard pulse signal with value 1 corresponding to 100% of communication packages delivered and 0 corresponding to no communication (0%), conveniently allows to achieve the desired switching dynamics of time-varying communication topology.

The following cumulative, Figure 21, illustrates the impact of the communication loss on the coordination performance; the loss factor is expressed through the percentage of perfect communication time, such that 90% corresponds to 10% of no communication time out of 10 sec period. The coordination performance is illustrated here by the ability to stabilize the separation between UAVs at coordination reference of 0.02 and the

resulting Euclidian separation. Figure 21 combines the results of seven simulations. For the convenience of comparison, the ideal communication results are also preserved.

Analysis of the results explicitly shows potentially severe adverse effect of loss of communication. Both subplots illustrate that minor communication losses up to 25% can be safely neglected; neither coordination states nor the separation distance dynamics are severely affected. This literally means that it is possible to lose about half of the communication but still be able to adhere to strict space separation constraints. This feature illustrates a necessary property of the proposed approach that consists of robustness of coordination to the communication loss. On the other hand, assuming the safe 3D separation established under ideal communication conditions to be $D_E = 150\ m$, establishes the minimum required communication bound that is consistent with the safety of flight at 25%.

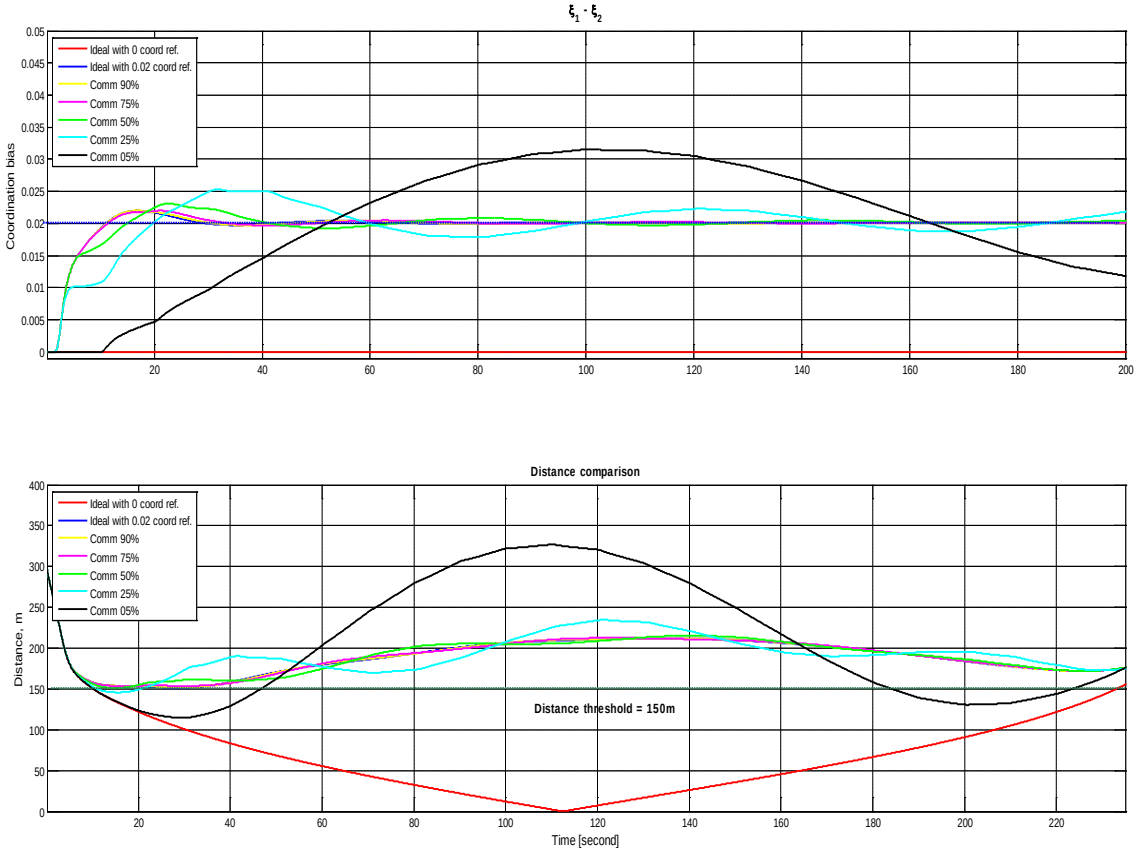

Figure 21. Impact of the communication loss on coordination performance.

The "price" of achieving the desired separation can be illustrated by the control efforts expressed in terms of the desired airspeed command and the speed-following dynamics. The cumulative picture of the actual speed profiles corresponding to the simulated scenarios is presented next in Figure 22. Their analysis shows that all speed profiles are feasible for execution; the actual speed profiles never reach the saturation limits of the velocity channel that were chosen for the UAV at hand [15, 30] *m/s*. However, the most important observation is that successful (communication from 100% to 50%) coordination does not impose any significant constraints or requirements on the propulsion system of UAVs, thus making the entire CPF approach readily feasible for onboard implementation.

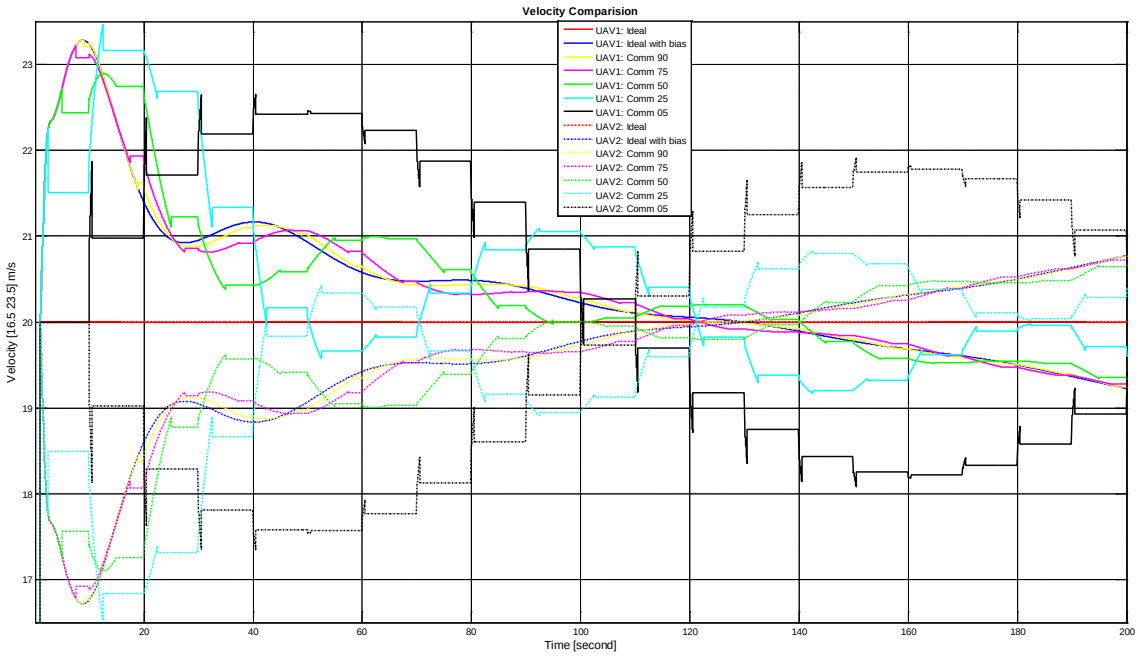

Figure 22. Control efforts expressed in terms of desired speed profile.

B. OVERVIEW OF NUMERICAL RESULTS

Based on the analysis of numerical experiments it can be concluded that the CPF concept is a viable and effective approach to automatically establish the safety of flight. Under nominal flight dynamics conditions, the features of the approach include a possibility of explicit separation of the PF from the coordination. On one hand, this

allows significant simplification of the path-planning phase of numbers of airplanes in the same airspace; the path-generation task is known to be NP hard. On the other hand, the separation of coordination task enables implementation and tuning of the coordination control law onboard particular UAVs, taking into account their specific constraints of the propulsion system and the autopilot limitations.

The results in particular demonstrate efficacy and robustness of the coordination law to a significant degree of communication degradation. Although the results obtained are specific to the particular class of UAVs, they still allow for generalization. The robust margins of the coordination performance already allow for up to 50% of communication loss without imposing and flight safety concerns.

Finally, although results obtained are encouraging and look promising for onboard implementation, it is still necessary to extend the scope of the effects capable to adversely affect the coordination performance. Among them are the degradation (complete loss or increase in information noise) of measurements across the entire INS/GPS system, including but not limited to the loss of GPS precision (due to aggressive maneuvering), flight control subsystem failure (actuators and control surfaces failure), errors in the UAV model identification, and many others.

V. CONCLUSION AND FUTURE WORK

A. CONCLUSION

The purpose of this thesis is to explore the current theories and enabling technologies, to practically implement the CPF algorithm for multiple UAVs, and to evaluate the impact of degraded communication during an assigned mission. One of the most important duties of a human pilot in the cockpit is to perform the function of See and Avoid in order to avoid a collision. Since a UAV has no one in the cockpit, the only possible way to acquire proper Search (or sensing) and Avoid functionality to the same degree as manned See and Avoid is a means of "communication." The ability to communicate with the other UAVs and the control station is the most critical factor for any UAV in the airspace, and significantly contributes the probability of a MAC.

In this thesis, the CPF algorithm is implemented. A PF algorithm is great for a single UAV, generating a path, and following the assigned path with carrying one single objective of the mission. In turn, CPF is a critical coordination technology, which enables exchanging the state information in real time and enables communication with the rest of fleet in a time-varying communications network. However, any interruption, fluctuation, or disturbance in the network is common. Therefore, the performance of a UAV can be measured by its responsiveness and ability to change speed when communication is degraded. As a result, the probability of collision is commonly affected by the performance of a UAV that has limited communication.

The simulation results clearly demonstrate the importance of communication by evaluating the relationships among the degradation of communication, the velocity responsive, and distance threshold. The robust margin of the CPF performance allows for up to 50% of communication loss without imposing any flight safety concerns. In fact, loss of communication is critical, even though the risk of degradation can be overcome or at least compensated by designing a robust responsive algorithm such as the current CPF algorithm.

B. FUTURE WORK

To safely merge UAVs into the National Airspace System safely, additional research is recommended, including actual field flight tests to compare and verify the simulation result, and the robustness of the design. The future work might explore the swarming level communication issues with a large fleet of vehicles. Moreover, the degraded communication scenario is an ongoing challenge for the modern technological working environment. Therefore, this idea can be extended to the field of any autonomous vehicles, such as ground robots and underwater unmanned systems, with only minor adjustments.

C. RECOMMENDATION

UAS have become a new customer in the National Airspace System and are coming into our daily life sooner than expected and planned. In fact, the U.S. Air Force is training more drone “pilots” than the traditional cockpit pilots. Unmanned systems have already assumed several risky tasks that humans are either incapable of doing or are too dangerous to perform. Moreover, these technologies are maturing and their capabilities are significantly increasing every day. It is obvious that unmanned systems will be an increasingly important part of our future Naval Aviation.

For Naval Aviation Maintenance Duty Officers, there are a few additional considerations for our near future Naval Aviation Enterprise. First, like the FAA’s expectation, the Naval Aviation Enterprise will share the missions and operations with unmanned systems. Changing our culture of the operation, including human behavior on the flight deck, will be a most challenging task. Even if we changed our policies, procedures and protocols in one day, it is impossible to change the culture and the behavior of sailors on an aircraft carrier in one day. The success of emerging UAS into our airspace severely depends on the culture of the Naval Aviation Enterprise. The culture has to catch up with the technology. It may take a very long time to place the right culture in the right place at the right time. Second, the field of UAV studies is one of highly advanced technology. Obviously, it is not easy to understand and acquire a certain

level of experience and knowledge in a short time. The community should start investing in and establishing a pool of future aviation maintenance professionals focused on UAS.

Unlike manned aircraft, unmanned systems are much more software-intensive systems. In addition, no longer will a pilot be required to walk into the maintenance department and describe a discrepancy upon completion of the flight. About one half of troubleshooting related to manned aircraft is completed at the desk of the maintenance control with a pilot's clear expression of the issues. On the other hand, a UAS is not able to describe the exact problems with the flight condition such as weather, symptom of the issues, and performance and response of aircraft. It can only provide formatted error codes. Therefore, troubleshooting in UAS requires a certain level of experience and a sophisticated understanding of the system. As a result, a technician and a maintenance manager are required to be familiar with the system and software-intensive nature of the troubleshooting.

Finally, based on the discussion in Chapter I, the probability of UAV mishap is much higher than the probability of manned aircraft mishap. To improve the quality of the UAV program in the U.S. Navy, a new investigation technique needs to be developed because the interview method will not be effective. Therefore, a highly educated maintenance professional will have more responsibilities and be more involved in unmanned mishap investigation. As a result, the early investment will significantly reduce the cost of total ownership of the sophisticated unmanned program in the near future.

THIS PAGE INTENTIONALLY LEFT BLANK

LIST OF REFERENCES

Biggs, N. (1993). *Algebraic graph theory*. New York, NY: Cambridge Univ. Press.

Cichella, V., Xargay, E., Dobrokhodov, V., Kamineer, I., Pascoal, M., & Hovakimyan, N. (2011). Geometric 3D path-following control for a fixed-wing UAV on SO(3). *AIAA Guidance, navigation and control conference*. Portland, OR. AIAA-2011-6415.

Contarino, M. (2009). "All Weather Sense and Avoid System for UASs: Task 3.1-Review and Analysis of Available System Technology Options and Justification For System Selection," 2009, December 5. Retrieved from http://www.scirellc.com/AWSASReport.pdf

Dobrokhodov, V. N, Kaminer, I. I., Jones, K. D., & Ghabcheloo, R. "Vision-Based Tracking and Motion Estimation for Moving Targets Using Small UAVs," AIAA Journal of Guidance, Control and Dynamics, 31(4), 2008.

Dobrokhodov, V. N., Yakimenko, O. A., Jones, K. D., Kaminer, I. I, Bourakov, E. Kitsios, I., & Lizarraga, M. "New Generation of Rapid Flight Test Prototyping System for Small Unmanned Air Vehicles," AIAA Modeling and Simulation Technologies Conferences and Exhibits. 2007, August 20-23, Hilton Head, SC.

Department of Defense (2004). Unmanned Aerial Vehicles and Uninhabited Combat Aerial Vehicles. Washington, D.C.: Defense Science Board. Retrieved from http://www.fas.org/irp/agency/dod/dsb/uav.pdf

Department of Transportation (2012). *FAA aerospace forecast*: Fiscal years 2012-2032. Washington, D.C.: Federal Aviation Administration. Retrieved from http://www.faa.gov/about/office_org/headquarters_offices/apl/aviation_forecasts/aerospace_forecasts/2012-2032/media/2012%20FAA%20Aerospace%20Forecast.pdf

Gertler, J. (2012). *U.S. unmanned aerial systems*. Congressional Research Service. Retrieved from http://fpc.state.gov/documents/organization/180677.pdf

Hodge, N. (2011, August 17). U.S. says drone, cargo plane collide over Afghanistan. *Wall Street Journal.* Retrieved from http://online.wsj.com/article/SB10001424053111903480904576512081215848332.html?mod=googlenews_wsj

Houry, J. K. (n.d) *Application to Graph Theory*. Ontario, Canada: University of Ottawa. Retrieved from http://aix1.uottawa.ca/~jkhoury/graph.htm

Jackson, J., Bencatel, R., Hasan, Z., and Girard, A. (2009, August 10-13) Stochastic patrolling and collision avoidance for two UAVs in a base defense scenario. AIAA Guidance, Navigation, and Control Conference. Chicago, IL.

Joint Planning and Development Office (JPDO). (n.d.) Next generation air transportation system international strategy. Retrieved from http://www.jpdo.gov/library/InformationPapers/JPDO_International%20Strategy.pdf

Joint Planning and Development Office (JPDO) (2011, January 4). Operating unmanned aircraft systems in 2018 and beyond: NextGen challenges and opportunities. Retrieved from http://www.jpdo.gov/newsarticle.asp?id=146

Lacher, A., Zeitlin, A., Maroney, D. Markin, K., Ludwig, D., and Boyd, J. (2010). Airspace Integration Alternatives for Unmanned Aircraft. AUVSI's Unmanned Systems Asia-Pacific 2010. February 1, 2010, Singapore.

McGarry, B. (2012, June 17). Drones most accident-prone U.S. Air Force craft: BGOV Barometer. *Bloomberg.com*. Retrieved from http://www.bloomberg.com/news/2012-06-18/drones-most-accident-prone-u-s-air-force-craft-bgov-barometer.html

Ren, W., Beard, R. W. & Atkins, E. M. Information consensus in multivehicle cooperative control, *Control Systems, IEEE* 27, no. 2, 71-82, April 2007 doi: 10.1109/MCS.2007.338264. Retrieved from http://ieeexplore.ieee.org/stamp/stamp.jsp?tp=&arnumber=4140748&isnumber=4140731

Under Secretary of Defense (AT&L) (2011, June 6) Mishap notification, investigation, reporting and record keeping (DoD Instruction 6055.07). Washington, DC: DoD. Retrieved from http://www.dtic.mil/whs/directives/corres/pdf/605507p.pdf

Weibel, R. E., & Hansman, R. J. (2005). *Safety considerations for operation of unmanned aerial vehicles in the national airspace system.* Cambridge, MA: MIT International Center for Air Transportation. Retrieved from http://dspace.mit.edu/bitstream/handle/1721.1/34912/Weibel%20-%20ICAT%20Report%20-%20UAV%20Safety.pdf

Xargay, E., Kaminer, I., Pascoal, A., Hovakimyan, N., Dobrokhov, V., Cichella, V., Aguiar, A., and Ghabcheloo, R. Time-critical cooperative path following of multiple UAVs over time-varying networks. *AIAA Journal*.

Xargay, E., Dobrokhodov, V., Kaminer, I., Pascoal, A., Hovakimyan, N., & Cao, C. (2012). Time-critical cooperative control of multiple autonomous vehicles. *IEEE Control Systems Magazine*, 49-73.

Z. Li., N. Hovakimyan, V. Dobrokhodov. “Vision-based Target Tracking and Motion Estimation Using a Small UAV,” 49th IEEE Conference on Decision and Control, 2010, December 15-17, Atlanta, GA.

THIS PAGE INTENTIONALLY LEFT BLANK

INITIAL DISTRIBUTION LIST

1. Defense Technical Information Center
   Ft. Belvoir, Virginia

2. Dudley Knox Library
   Naval Postgraduate School
   Monterey, California

3. Raymond R. Jr. Buettner
   Naval Postgraduate School
   Monterey, California

4. Vladimir N. Dobrokhodov
   Naval Postgraduate School
   Monterey, California

5. Kevin D. Jones
   Naval Postgraduate School
   Monterey, California

6. Dan C. Boger
   Naval Postgraduate School
   Monterey, California